

F/G 20/5

STABILITY OF A NORMAL SHOCK IN RADIAL REACTING FLOW WITH NONUNI--ETC(U)

JUN 81 D A DURRAN, M EPSTEIN, W R WARREN

F04701-80-C-0081

UNCLASSIFIED

TR-0081(6940-01)-7

R. WARREN
SD-TR-81-51

NL

ΔG°
ΔG° = -306 J

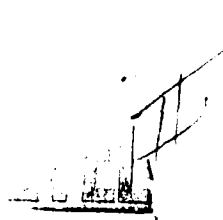
END

DAIF

FILED

9 81

OTIC 0

 (12) BS

AD A103066

Stability of a Normal Shock in Radial Reacting Flow with Nonuniformities

D. A. DURRAN, M. EPSTEIN, and W. R. WARREN, JR.
Aerophysics Laboratory
The Aerospace Corporation
El Segundo, Calif. 90245

15 June 1981

DTIC
ELECTE
AUG 19 1981
S D A

APPROVED FOR PUBLIC RELEASE;
DISTRIBUTION UNLIMITED

DTIC FILE COPY

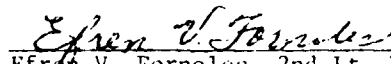
Prepared for
SPACE DIVISION
AIR FORCE SYSTEMS COMMAND
Los Angeles Air Force Station
P.O. Box 92960, Worldway Postal Center
Los Angeles, Calif. 90009


81 8 19 056

This report was submitted by The Aerospace Corporation, El Segundo, CA 90245, under Contract No. F04701-80-C-0081 with the Space Division, Deputy for Technology, P.O. Box 92960, Worldway Postal Center, Los Angeles, CA 90009. It was reviewed and approved for The Aerospace Corporation by W. R. Warren, Jr., Director, Aerophysics Laboratory. 2nd Lt Efren V. Fornoles, SD/YLXT, was the project officer for the Mission-Oriented Investigation and Experimentation (MOIE) program.

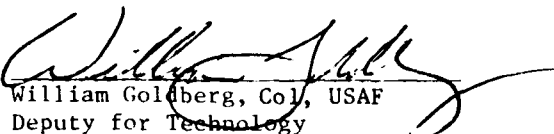
This report has been reviewed by the Public Affairs Office (PAS) and is releasable to the National Technical Information Service (NTIS). At NTIS, it will be available to the general public, including foreign nations.

This technical report has been reviewed and is approved for publication. Publication of this report does not constitute Air Force approval of the report's findings or conclusions. It is published only for the exchange and stimulation of ideas.


Efren V. Fornoles, 2nd Lt, USAF
Project Officer


Florian P. Meinhardt, Lt Col, USAF
Director of Advanced Space Development

FOR THE COMMANDER


William Goldberg, Col, USAF
Deputy for Technology

UNCLASSIFIED

SECURITY CLASSIFICATION OF THIS PAGE (When Data Entered)

REPORT DOCUMENTATION PAGE		READ INSTRUCTIONS BEFORE COMPLETING FORM
1. REPORT NUMBER SD-TR-81-51	2. GOVT ACCESSION NO. AD-A103	3. RECIPIENT'S CATALOG NUMBER 066
4. TITLE (and Subtitle) STABILITY OF A NORMAL SHOCK IN RADIAL REACTING FLOW WITH NONUNIFORMITIES		5. TYPE OF REPORT & PERIOD COVERED 1
		6. PERFORMING ORG. REPORT NUMBER TR-0081(6940-01)-7
7. AUTHOR(s) Donald A. Durran, Melvin Epstein, and Walter R. Warren, Jr.		8. CONTRACT OR GRANT NUMBER(s) F04701-80-C-0081
9. PERFORMING ORGANIZATION NAME AND ADDRESS The Aerospace Corporation El Segundo, Calif. 90245		10. PROGRAM ELEMENT, PROJECT, TASK AREA & WORK UNIT NUMBERS
11. CONTROLLING OFFICE NAME AND ADDRESS Space Division Air Force Systems Command Los Angeles, Calif. 90009		12. REPORT DATE 15 June 1981
		13. NUMBER OF PAGES 60
14. MONITORING AGENCY NAME & ADDRESS (if different from Controlling Office)		15. SECURITY CLASS. (of this report) Unclassified
		15a. DECLASSIFICATION/DOWNGRADING SCHEDULE
16. DISTRIBUTION STATEMENT (of this Report) Approved for public release; distribution unlimited		
17. DISTRIBUTION STATEMENT (of the abstract entered in Block 20, if different from Report)		
18. SUPPLEMENTARY NOTES		
19. KEY WORDS (Continue on reverse side if necessary and identify by block number) Chemical Laser Radial Flow Cylindrical Laser Reacting Flow Normal Shock Pressure Recovery		
20. ABSTRACT (Continue on reverse side if necessary and identify by block number) Pressure recovery for a cylindrical chemical laser is optimized when a normal shock is located just outside the optical cavity region. The feasibility of maintaining a shock in such a position when the radial flow is reacting and contains nonuniformities has been demonstrated in a small-scale experiment. Flow visualization and flow diagnostics have verified that the shock is stable and that its position is readily adjusted by changing the downstream pressure. Although actual pressure recovery was not measured, it is expected that 100%		

DD FORM 1473
(FACSIMILE)

UNCLASSIFIED

SECURITY CLASSIFICATION OF THIS PAGE (When Data Entered)

SECURITY CLASSIFICATION OF THIS PAGE(When Data Entered)

20. ABSTRACT (Continued)

A

SECURITY CLASSIFICATION OF THIS PAGE(When Data Entered)

PREFACE

The work reported herein had its beginning early in 1975 when the Air Force Weapons Laboratory (AFWL) sponsored a small-scale cylindrical laser experiment, the RASER (radial laser), at The Aerospace Corporation. The authors express their appreciation for the patience and encouragement of the AFWL personnel, in particular, Colonels J. Rich and D. Olson and Dr. L. Wilson.

We acknowledge the contribution of the many at Aerospace who have supported the effort over the years. In the laboratory machine shop R. L. Smith, E. A. Tucker, B. Perry, A. Wike, and H. Paul performed outstandingly to make the nozzle hardware. Thanks are due also R. Pedley (deceased), R. L. Lott and G. Bronson (consultant) for their contributions to our designs.

M. E. Gerard was in large part responsible for building the test facility and setting up the experiment. He was assisted by A. Wildvank, R. R. Valenzuela, J. T. Valero, and R. G. Aurandt. J. Narduzzi was responsible for most of the controls and instrumentation in the facility.

When the use of gaseous fluorine was required, R. E. Cook built a new handling system and has operated it throughout the test program without incident. Valuable technical support was provided by other members of the laboratory staff during the test phase. D. A. Storvick took high-speed color photographs of the chemiluminescent flow, E. F. Cross and O. L. Gibb recorded flow stability at various operating conditions with a high-sensitivity video system, G. I. Segal resolved complex pitot-pressure scans by averaging on a PDP11 computer, and R. H. Ueunten and Dr. A. Kwok (with Segal) obtained spectra from a very weak source for determining flow temperature and chemistry.

K. L. Foster assisted in the computer calculations using the DESALE and NEST codes, which served as the analytical basis for this experiment and for parametric studies of cylindrical lasers in general.

CONTENTS

PREFACE.....	1
I. BACKGROUND.....	7
II. TECHNICAL APPROACH.....	9
III. FABRICATION.....	15
IV. ALTERNATE APPROACH.....	21
V. COLD FLOW TESTS.....	25
VI. HOT FLOW TESTS.....	33
VII. REACTIVE FLOW TESTS.....	39
VIII. PRESSURE MEASUREMENTS.....	43
IX. TEMPERATURE MEASUREMENTS.....	55
X. CONCLUSIONS AND RECOMMENDATIONS.....	59

PRECEDING PAGE BLANK-NOT FILMED

FIGURES

1.	Experiment Setup.....	10
2.	Cylindrical Nozzle Design.....	11
3.	Calculated Performance.....	13
4.	Pressure Recovery vs Shock Position (nominal conditions).....	14
5.	Sample Nozzle Parts.....	16
6.	Coolant Passage Core Configuration.....	17
7.	Cerrobend Core Specimen.....	18
8.	Completed Electroformed Core.....	19
9.	Alternate Nozzle Design.....	22
10.	Alternate Nozzle Layout.....	23
11.	Alternate Nozzle (prior to final assembly).....	24
12.	Sample Nozzle for Core Flow Tests.....	26
13a.	Axial Scan Across Oxidizer Jet; $R = 1 \text{ mm}$, $p_o = 1 \text{ atm}$	27
13b.	Axial Scan Across Fuel Jet; $R = 1 \text{ mm}$, $p_o = 1 \text{ atm}$	28
14.	Circumferential Scan Around Oxidizer Jets; $p_o = 1 \text{ atm}$, $p_e = 12 \text{ Torr}$	29
15.	Nozzle Assembly.....	30
16.	Cold Flow Test, Axial Pitot Pressure Scan at $R = 0.5 \text{ mm}$	31
17.	Nonreacting Flow Conditions.....	34
18.	Nitrogen Heater.....	35
19.	Combustor-Nozzle Configuration.....	36
20.	Chemiluminescence Photographs.....	40
21.	Reacting Flow Test, Axial Pitot Pressure Scan at $R = 2 \text{ mm}$	44
22.	Pitot Pressure Above Nozzle No. 7, $p_c = 14 \text{ Torr}$	45

FIGURES (Continued)

23a.	Oxidizer Nozzle Characteristics, $\gamma = 1.4$	46
23b.	Fuel Nozzle Characteristics, $\gamma = 1.4$	47
24.	Computer Averaged Results, $p_c = 14$ Torr.....	48
25.	"Zone of Silence" Results.....	50
26.	Pitot-Static Pressure Probe.....	52
27.	Results of Pitot-Static Measurements.....	53
28.	Rotational Temperature Test Setup.....	56
29.	Rotational Temperature and HF($v = 3$) [$T \pm 50$ K, relative HF($v = 3$) $\pm 10\%$].....	57
30.	Cylindrical Chemical Laser Cylindrical Shock Pressure Recovery....	61

I. BACKGROUND

With the advent of high-powered chemical lasers operating at cavity pressures of 10 to 20 Torr, considerable attention has been given the pressure recovery in a supersonic diffuser attached to these devices.¹⁻⁵ The large amount of chemical energy released in the diffuser makes the design critical, because good pressure recovery can ordinarily be obtained only for conditions where laser efficiency is low. Nevertheless, systems have been tested where 80% of the pressure recovery in a normal shock has been obtained for diffuser inlet Mach numbers of from 2 to 4 at practical laser operating conditions.

As the lasers increased in size, it was expedient to change from a linear to a cylindrical configuration. Instead of having a very long nozzle assembly with a long cavity, the nozzle is arranged in a cylindrical fashion so that the cavity is an annulus. However, other aspects of the laser are complicated by such an arrangement, for example, the optics required to couple to an annular gain region. The diffuser for the cylindrical laser, although not intrinsically different from that for a linear laser, becomes very large in weight and volume. For this reason, the possibility of operating a cylindrical laser without a supersonic diffuser has been considered.

We propose that a normal shock in the radial flow be located downstream of the cavity, the position of which is established by the back-pressure level

¹W. R. Warren, Jr., Reacting Flow and Pressure Recovery Processes in HF/DF Chemical Lasers, TR-0074(9240-02)-1, The Aerospace Corporation, El Segundo, Calif. (30 November 1973).

²D. G. Hook et al., HF/DF Chemical Laser Technology Studies, AFWL-TR-74-150, TRW, Inc., Redondo Beach, Calif. (October 1974).

³D. A. Durran and S. W. Liu, Pressure Recovery in a Constant-Area Diffuser for Chemical Lasers with Nozzle Base Relief, TR-0075(5533)-3, The Aerospace Corporation, El Segundo, Calif. (30 June 1975).

⁴R. I. Teper and H. A. Arbit, Chemical Laser Advanced Diffuser/Ejector, RI/RD-78-102, Rocketdyne Division, Rockwell International (January 1978).

⁵F. R. Zumpano, R. N. Guile, and W. A. Eckerle, Vaned Diffuser and Supersonic/Supersonic Ejector Screening Investigations, TR-R80-914767-1, United Technology Research Center, East Hartford, Connecticut (June 1980).

in the exhaust ducting (at or near ambient). This is analogous to the normal shock standing in the expanding section of a supersonic nozzle, which again is caused by the back-pressure level. Obviously, the position of the shock would automatically adjust to different radii (area ratio positions) as the back pressure varies; thus, in practice, the system offers a simple, lightweight pressure-recovery technique that would passively adjust itself to permit operation over an appreciable range of ambient pressures (i.e., altitudes). The feasibility question that is being asked is, "Will such a normal shock structure be stable in reacting radial flow?" In addition, the influence on stability of nonuniformities in the flow coming from a typical laser nozzle must be assessed.

An experiment that was performed to answer these questions is described in this report. It was hoped that the results, if favorable, would be useful in guiding the development programs for large cylindrical lasers.

II. TECHNICAL APPROACH

In designing an experiment to demonstrate the stability of a normal shock in a reacting radial flow with nonuniformities, the scaling of the test device is very important. Obviously, a test in full-scale hardware would be most beneficial, but it would also be very expensive. Therefore, a small-scale experiment was planned with as many of the features of the full-scale hardware included as reasonably possible. The actual size (i.e., total flow rate) was limited by the facilities available.

Laser facilities in the laboratory were conceived for arc-heated devices with a total flow rate of about 25 g/sec at pressure levels of 5 to 10 Torr. Because it was desirable to simulate the cold-reaction HF laser, which operates with high levels of F-atom concentration ($\alpha = 1.0$ and $T_0 = 1800$ K), a nozzle with a total area of 91 cm^2 operating at 1 atm was selected. To keep end effects to a minimum, a length-to-diameter ratio of 2 for the inlet to the cavity was maintained. This would permit enough room in the body of the nozzle (it was hoped) to feed gases and cooling water from one end.

The general arrangement for the experiment is shown in Figure 1. The cylindrical nozzle, 3.8 cm in diameter and 7.6 cm long, is surrounded by a toroidal compression chamber that collects the reacting flow between end walls that can be adjusted in their spacing lengthwise and have a fixed 1.5-cm standoff from the nozzle. By adjusting the area of the exhaust from this chamber, a pressure can be established that will support a normal shock at the inlet (i.e., 1.5 cm above the nozzle). End flow that passes outside the compression chamber (as well as that exhausting from it) is collected in the test section and conveyed to the exhaust system. This arrangement can be compared to the full-scale system in that the flow through the shock would be passed to ambient pressure (or to the next stage of pumping), whereas the end flow would be energized with cavity purges and diffused or combined with the main flow.

The nozzle design selected for this experiment is shown in Figure 2. Although it is a compromise necessitated by the small scale of the experiment, it is essentially a slit design. That is, the dilute oxidizer and the fuel

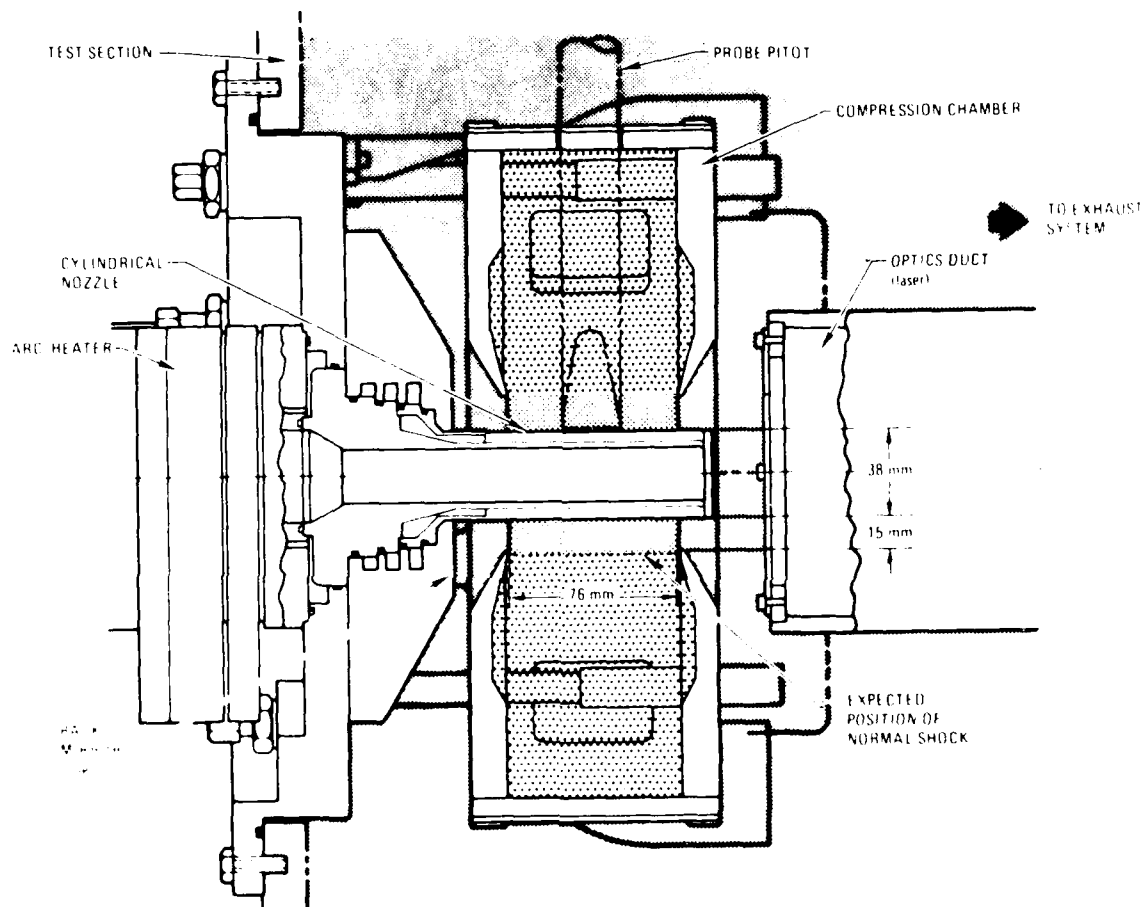


Figure 1. Experiment Setup

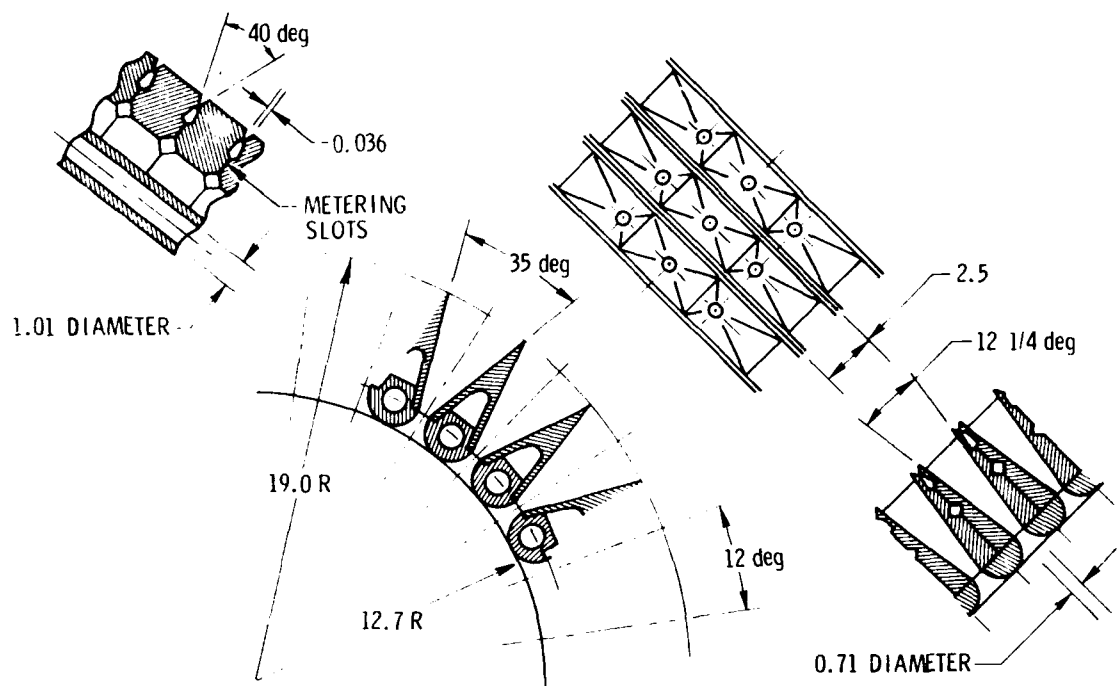


Figure 2. Cylindrical Nozzle Design

issue from adjacent slits such that nonuniformities are at right angles to the optical axis (i.e., axis of the nozzle). In the case of the oxidizer nozzle, there are individual circular throats that expand to rectangular exits, which form a contiguous flow around the periphery of the cylinder. This arrangement does produce nonuniformities in the direction of the optical axis as a result of boundary layers, but it is necessary in order to provide room for the fuel manifold and water cooling passages.

Calculated flow conditions for the cavity region of this nozzle are shown in Figure 3. These results were obtained with the use of the DESALE-3 computer code. Note that the nozzle operates with a mixed diluent (i.e., N_2 and He). It was determined in early tests of battleship hardware that the mixed diluent was required to get enough energy into the plenum gases with the arc heater that was available. The jump in conditions at 1.5 cm is due to the presence of a normal shock; conditions downstream of the shock were calculated with the use of the NEST computer code.

Several runs were made with NEST for the shock located at different positions, and the total downstream pressure versus shock position is plotted in Figure 4. The results indicate a decreasing total pressure with radial position, a necessary condition for normal shock stability. Any disturbance in the shock position will result in pressure changes in the flow that will restore the shock to its original position. Note that the sharp drop in total pressure as the flow expands permits the use of a pitot measurement to ascertain the position of the normal shock. In the subsonic region, the pitot pressure will be essentially constant. Also, the flow immediately downstream of the shock should be more luminous as a result of the higher temperature and increased rate of chemical reactions. Therefore, visual means can be used to verify the presence and stability of the normal shock.

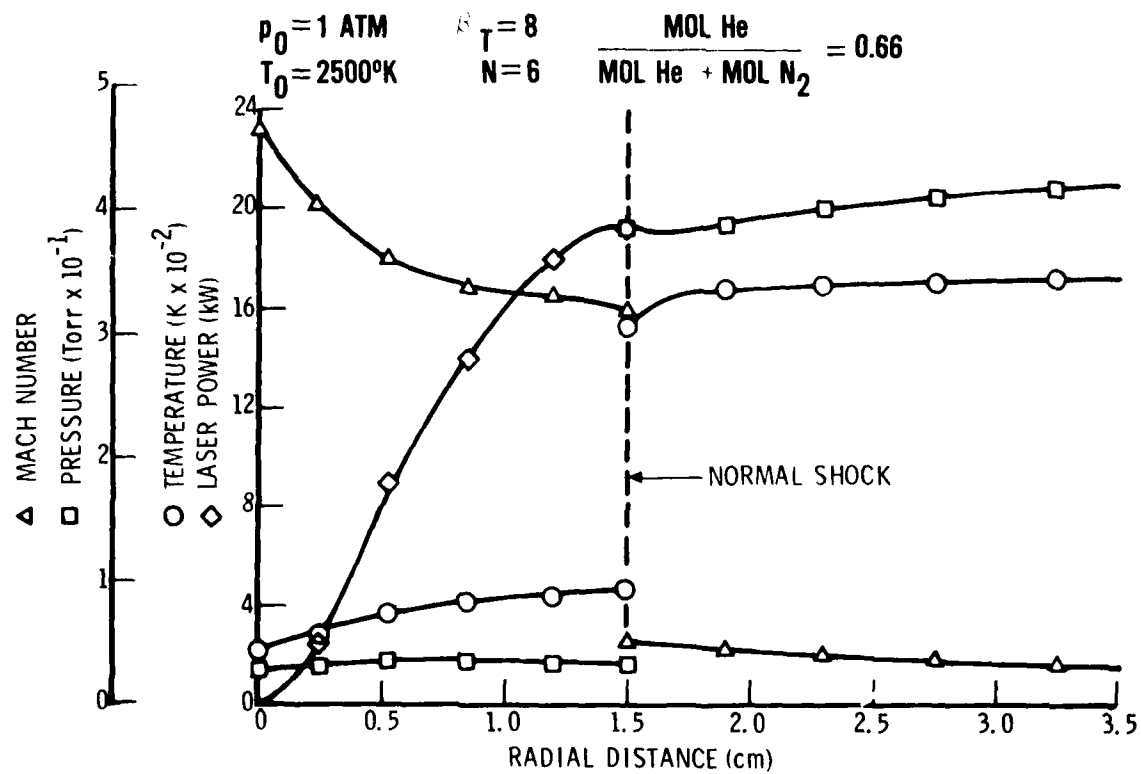


Figure 3. Calculated Performance

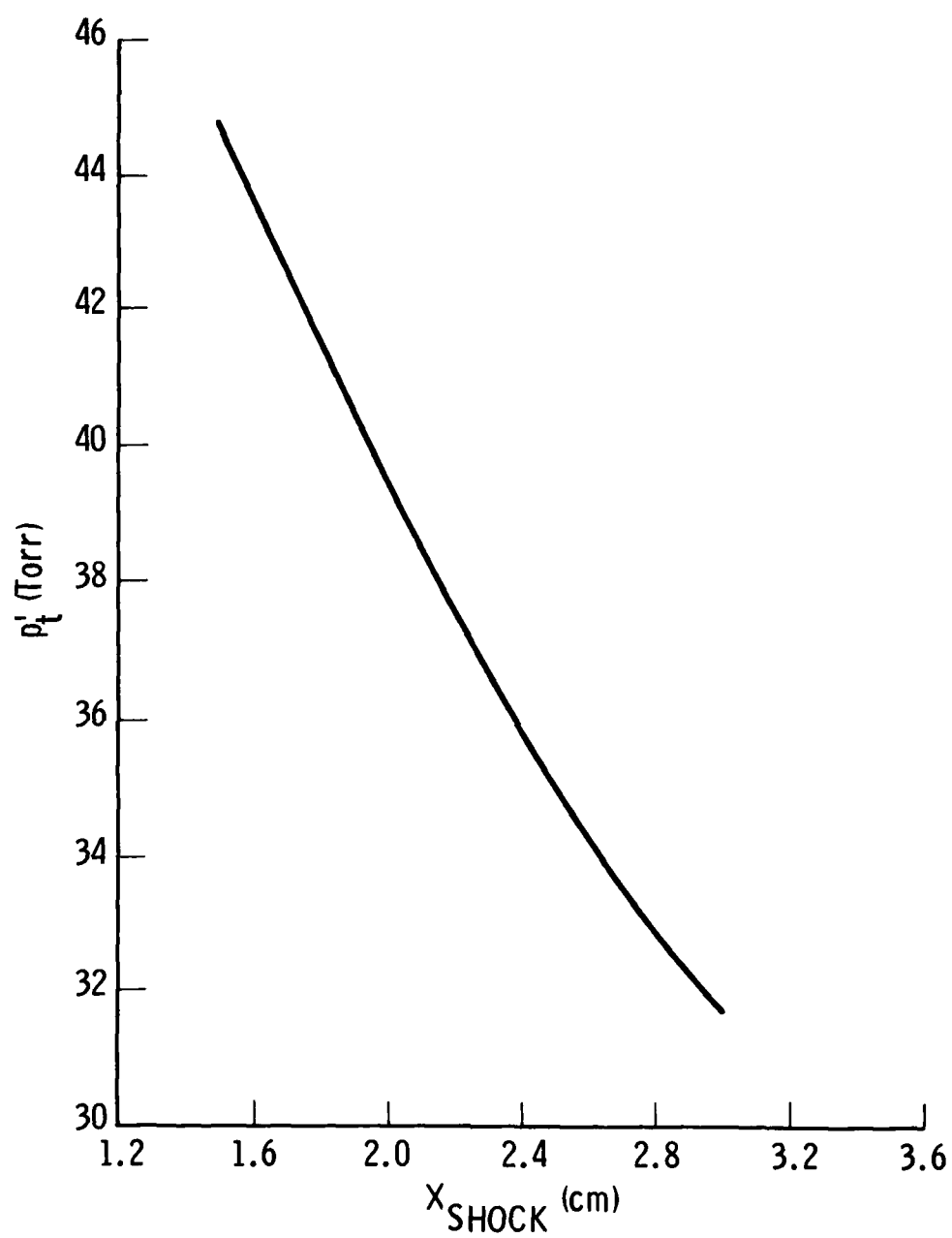


Figure 4. Pressure Recovery vs Shock Position (nominal conditions)

III. FABRICATION

It was obvious at the beginning of the program that the fabrication of the small cylindrical nozzle would be the critical item. The plan was to assemble the nozzle by soldering (450°F) washers that contained the expansion sections of the oxidizer nozzle and metering slits for the fuel manifold onto an electroformed core that contained the oxidizer throats and the cooling water passages. This arrangement is indicated in the photographs of Figure 5. These sample parts were made early in the fabrication cycle so that a flow test of the nozzle could be made to determine its characteristics. No cooling passages were required and are, therefore, not visible in Figure 5. (The inset in Figure 5 is a cross section of the core with the cooling passages in position.)

Great difficulty was experienced in coring the holes for the cooling water passages. Initially aluminum wire was used that had a small slot on the back side so the sodium hydroxide (Figure 6) used to remove them could be pumped through the entire length of the passage. Because the wires were not sealed in place, the electrolyte penetrated into these slots, leached out during the plating process, and inhibited the bond on the substrate material. Waxing of the cores was judged to be impractical because the design required a raised core configuration that could not be machined or cleaned. An attempt was made to use Cerrobend, a low-melting-point eutectic of bismuth and lead. Test specimens were made (Figure 7) that proved to be entirely adequate when subjected to a hydrotest at 2000 psi. A core was completed (Figure 8) but failed when the Cerrobend was melted out, probably because of the partial melting of the alloy in closed-off portions of the passages and the resultant expansion that induced very high stresses.

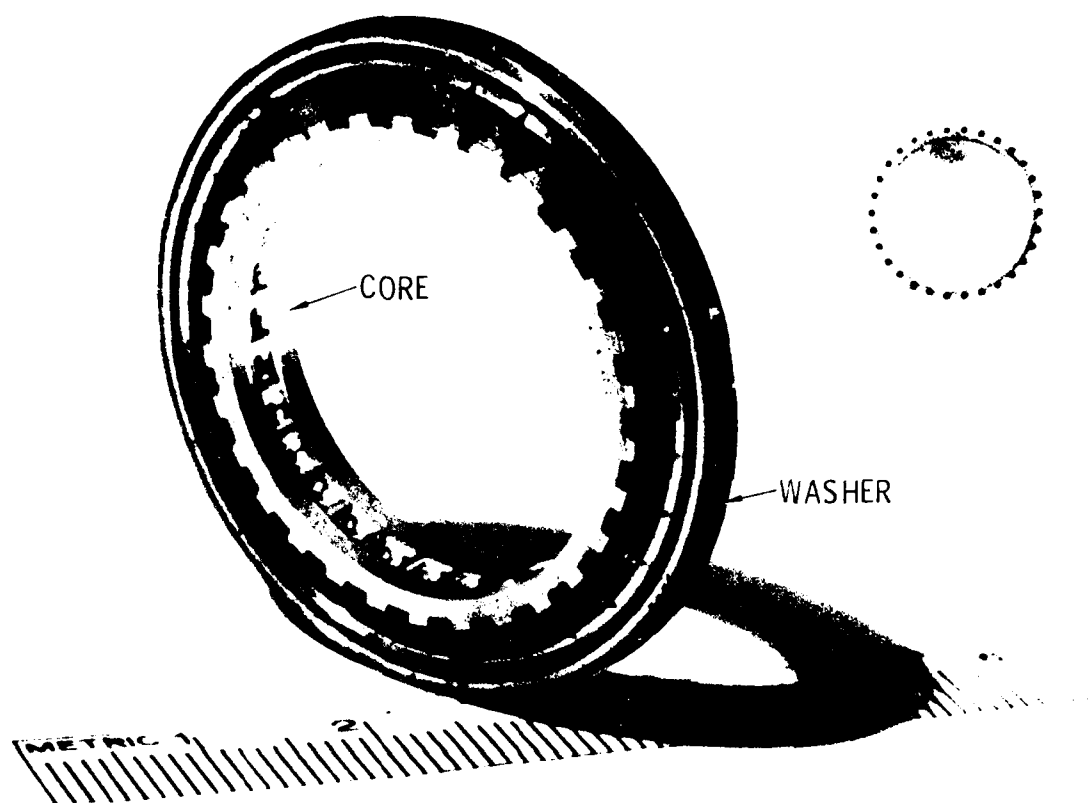
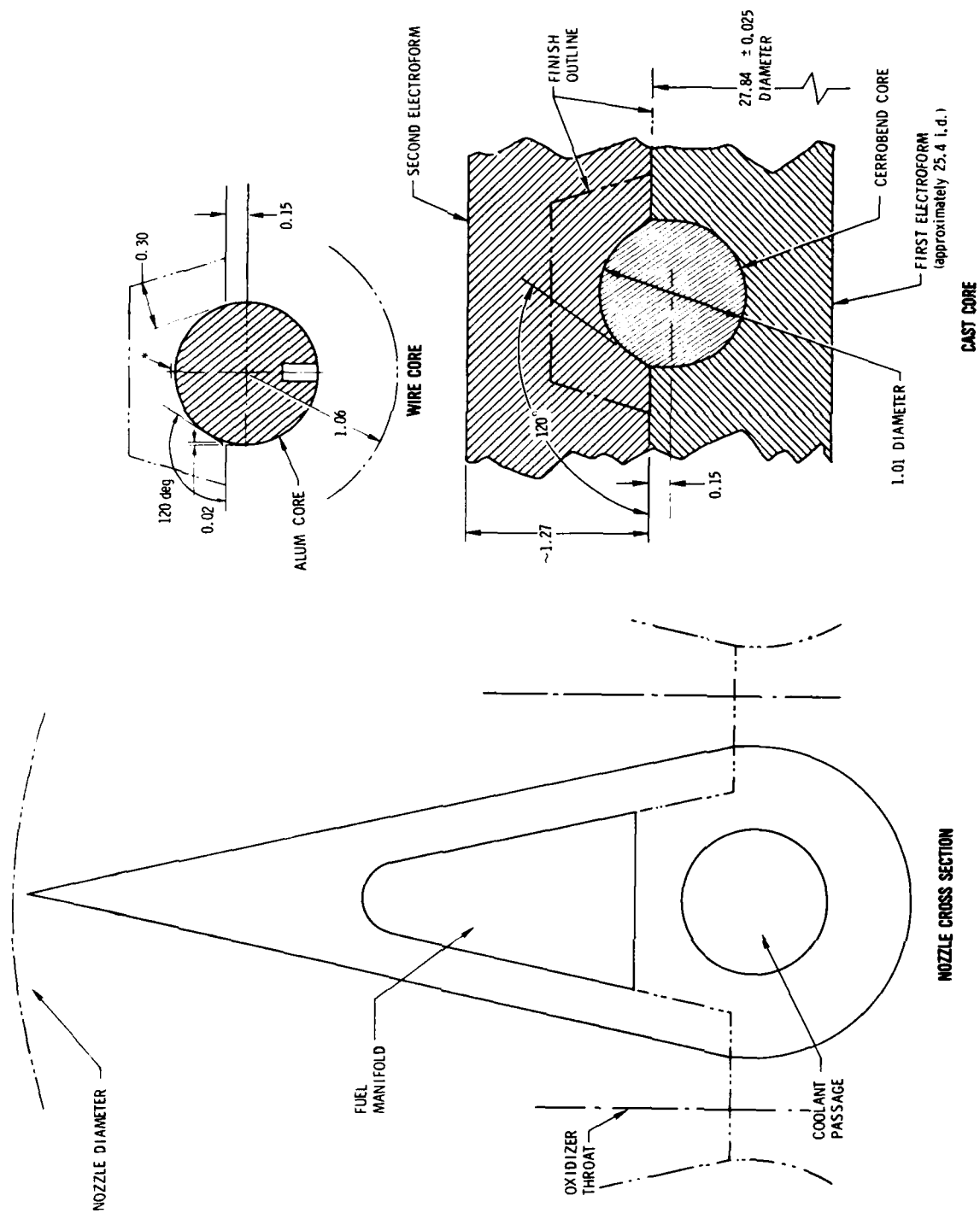


Figure 5. Sample Nozzle Parts



Dimensions in millimeters

Figure 6. Coolant Passage Core Configuration

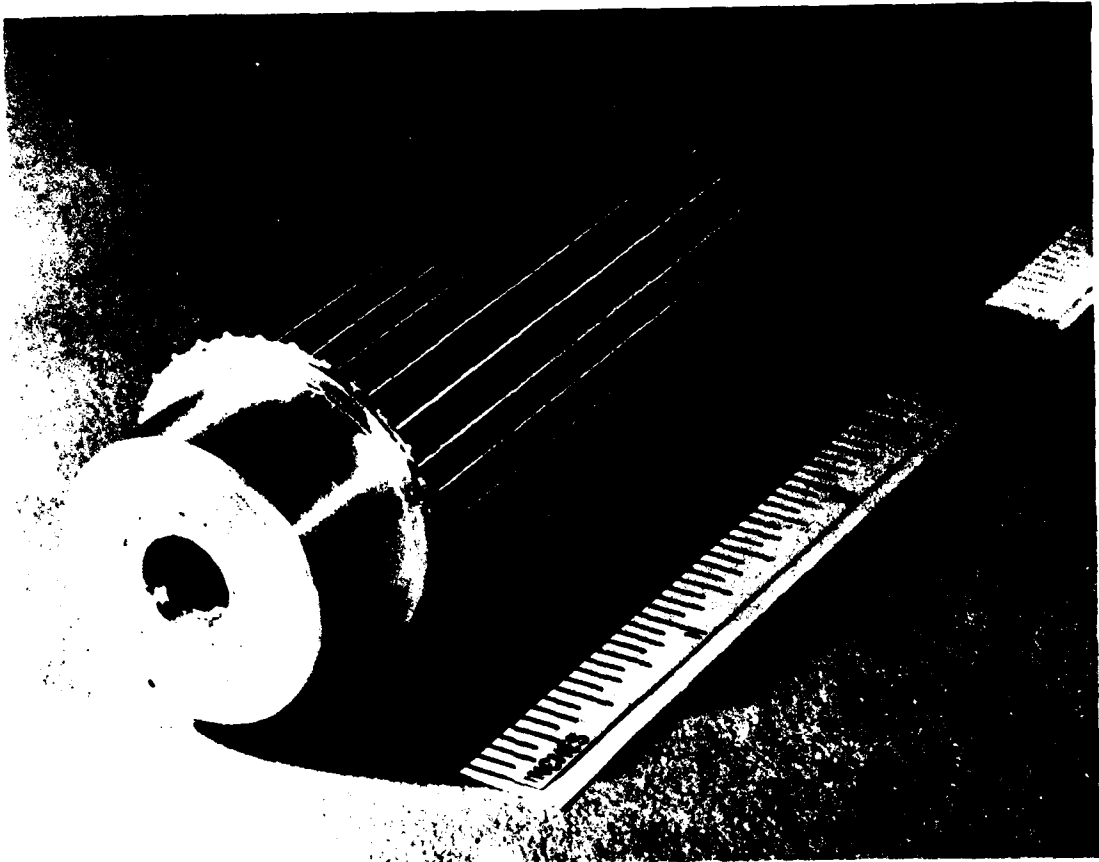


Figure 7. Cerrobend Core Specimen

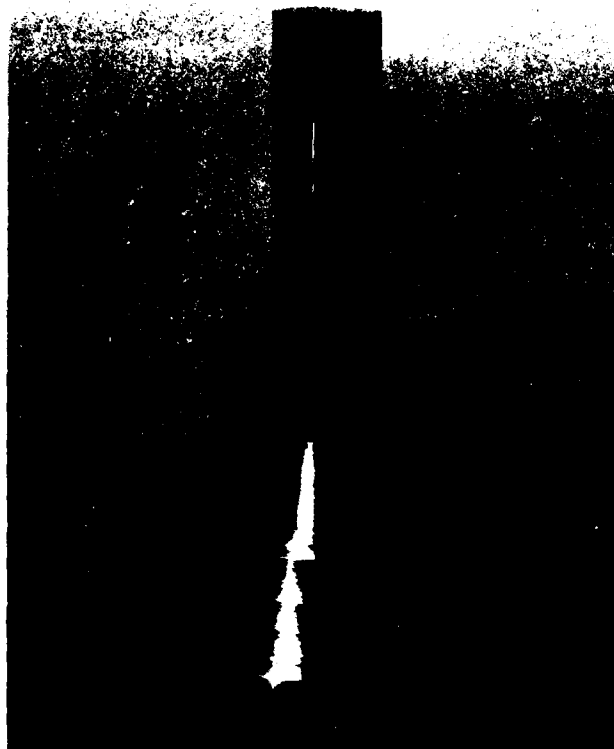
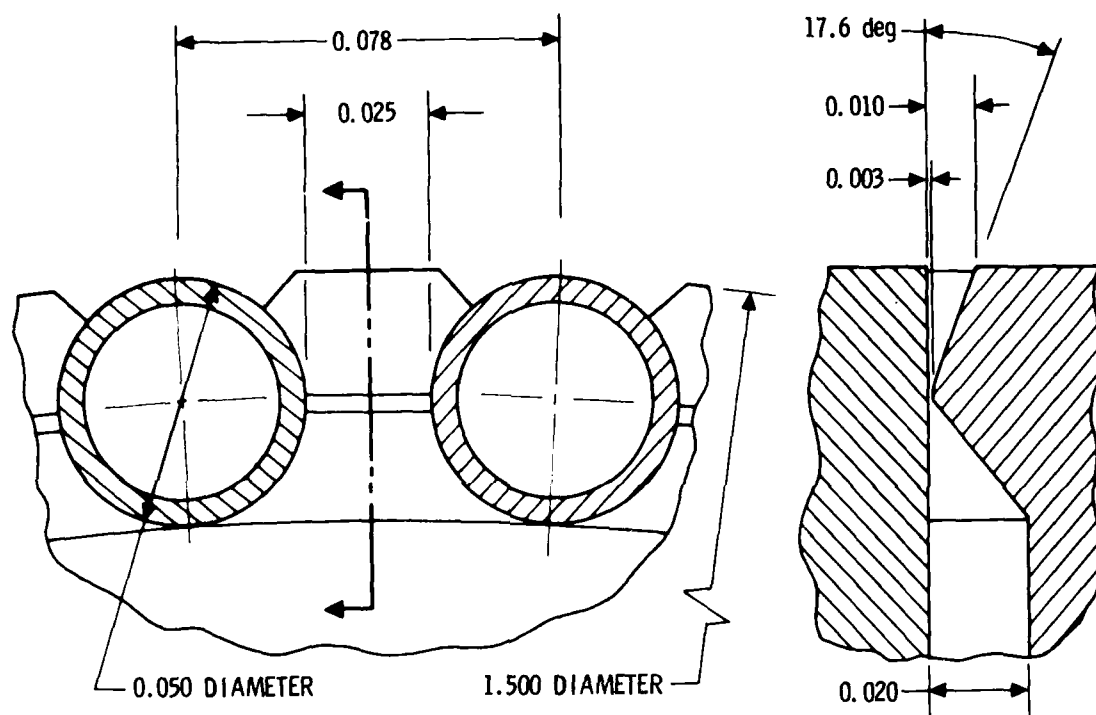


Figure 8. Completed Electroformed Core

IV. ALTERNATE APPROACH

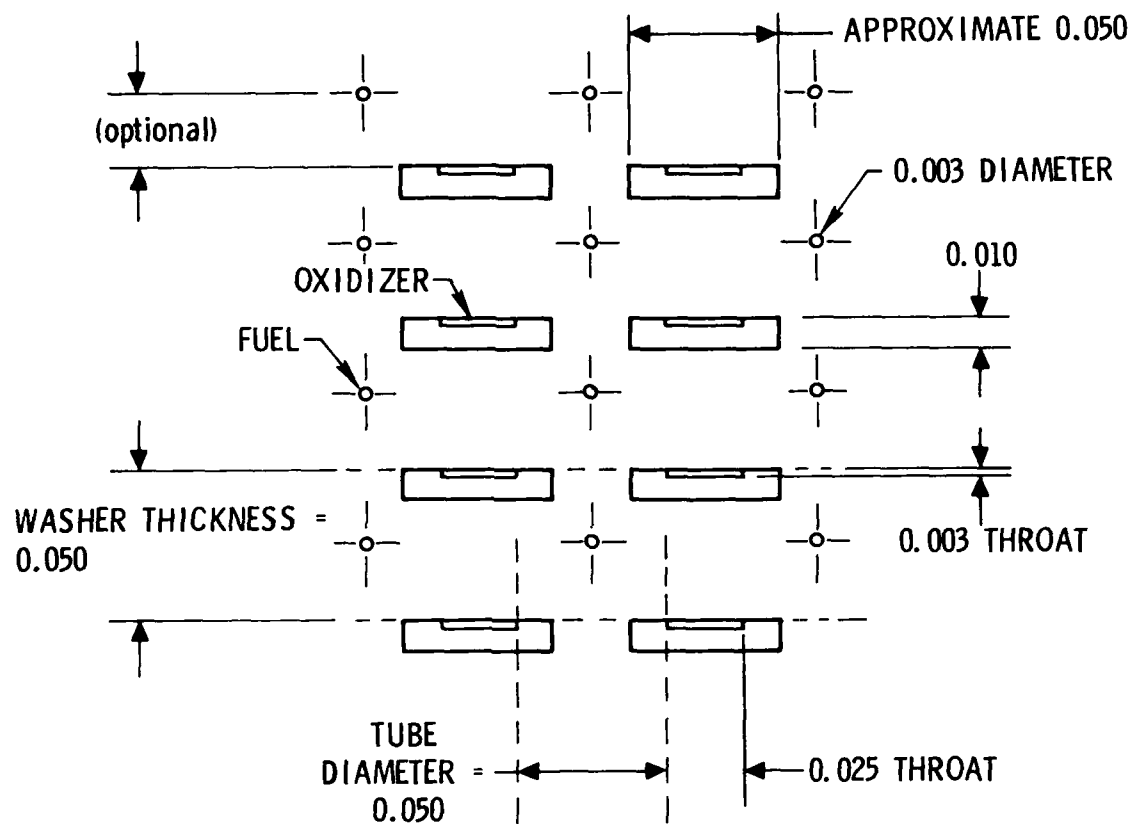
Because so much trouble was experienced in fabricating a nozzle with cooling water passages, an alternate approach was considered. The essential feature required for the demonstration of the stability of the normal shock was that the flow be chemically reacting and contain nonuniformities. Success had been achieved in the laboratory in obtaining stable flames in linear nozzle configurations using the chain reaction and initiating the reaction with nitric oxide (NO). These were low Mach-number flows with plenum conditions of 0.1 atm and 300 K. It seemed promising to consider using this technology in the normal shock experiment because the hardware could be uncooled and there would certainly be abundant heat released from the chain reaction. A simple nozzle design was required because so much time and expense had been expended in trying to fabricate the other nozzle. Furthermore, the chain reaction would require the use of gaseous fluorine. (Sulfur hexafluoride was the source of F-atoms in the arc-heated laser.)

A very crude nozzle design was selected and is shown in Figure 9. The oxidizer nozzle is formed by contours machined in nickel washers that are slipped over 60 stainless steel tubes. The spaces between the tubes and the washers provide the throats. Note that there is no seal between the tubes and washers (a simple mechanical fit), so the gases in the plenum can leak through crevices around the throat. Although very undesirable from the standpoint of a good nozzle, this arrangement made assembly and disassembly very easy. The stainless steel tubes are fuel manifolds that are provided with a small orifice at each oxidizer nozzle for the injection of the fuel. If this cylindrical nozzle arrangement was unrolled and laid out flat, the configuration would be as shown in Figure 10. It is obvious that there is a large amount of base area between nozzles and between oxidizer and fuel. This condition is not characteristic of good laser nozzle design, but would result in nonuniformities in the flow that would be a more severe test for shock stability. A photograph of the nozzle prior to assembly is shown in Figure 11.



Dimensions in inches

Figure 9. Alternate Nozzle Design



Dimensions in inches

Figure 10. Alternate Nozzle Layout

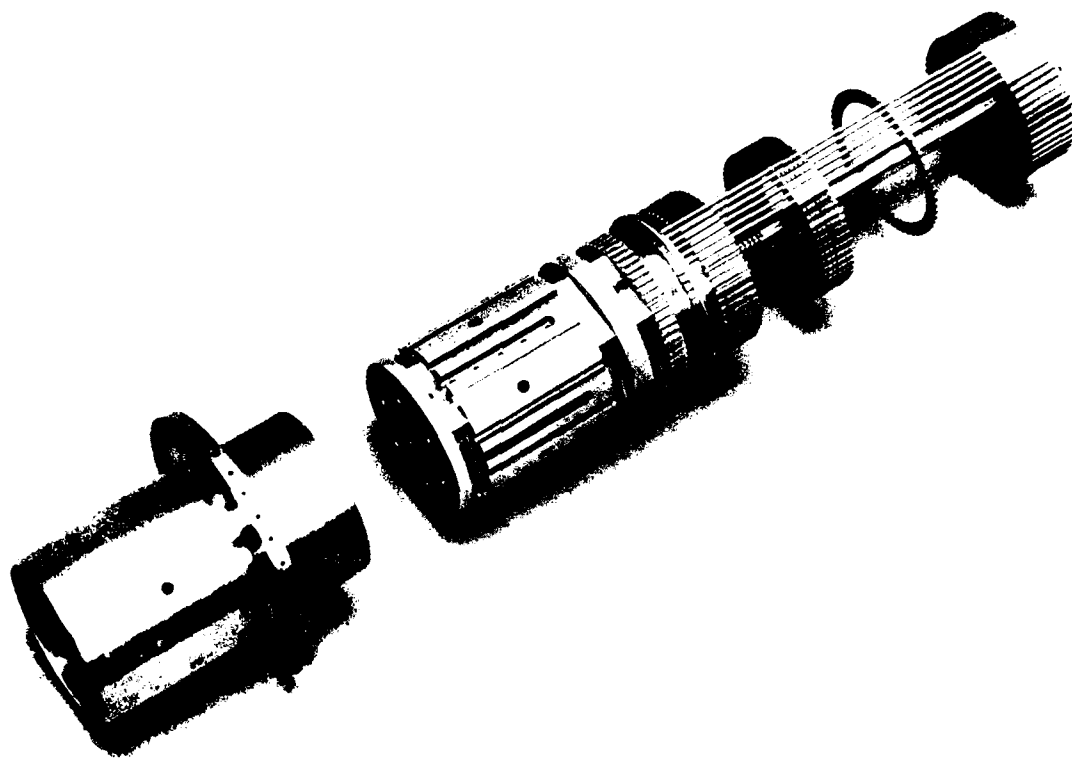


Figure 11. Alternate Nozzle (prior to final assembly)

V. COLD FLOW TESTS

Because the design of the nozzle was so unorthodox, a small sample assembly was fabricated for cold-flow tests (Figure 12). By means of pitot pressure measurements with an axial, a radial, and a circumferential traverse, the quality of the flow from the nozzle could be assessed. A typical axial scan across the oxidizer and fuel openings is shown in Figures 13a and 13b, respectively. A circumferential scan around the oxidizer openings is shown in Figure 14. It was apparent that the radial extent of the supersonic flow from the nozzle is a few millimeters, not the 1.5 cm expected from the other nozzle design. In addition, the large variations in the pitot pressure observed during the circumferential scan at 12 Torr indicated that the nonuniformities would indeed be very large.

The nozzle assembly was completed and is shown in Figure 15. It was mounted in the test section, and an axial pitot pressure scan across the 11 oxidizer openings at the center of the nozzle was made. The data taken at a radial position of 0.5 mm are shown in Figure 16. It was noted that the lowest back pressure that could be achieved with nominal flow rates (cold) and with the use of the maximum facility vacuum pumping capacity was approximately 15 Torr. It was expected that back pressure with reaction would be somewhat higher because of the high-temperature exhaust, so the supersonic portion of the flow would be further degraded. It was decided that the length of the nozzle assembly should be decreased by about 33% so that the mass flow could be reduced, reducing the back pressure on the flow by a small amount (4 or 5 Torr).

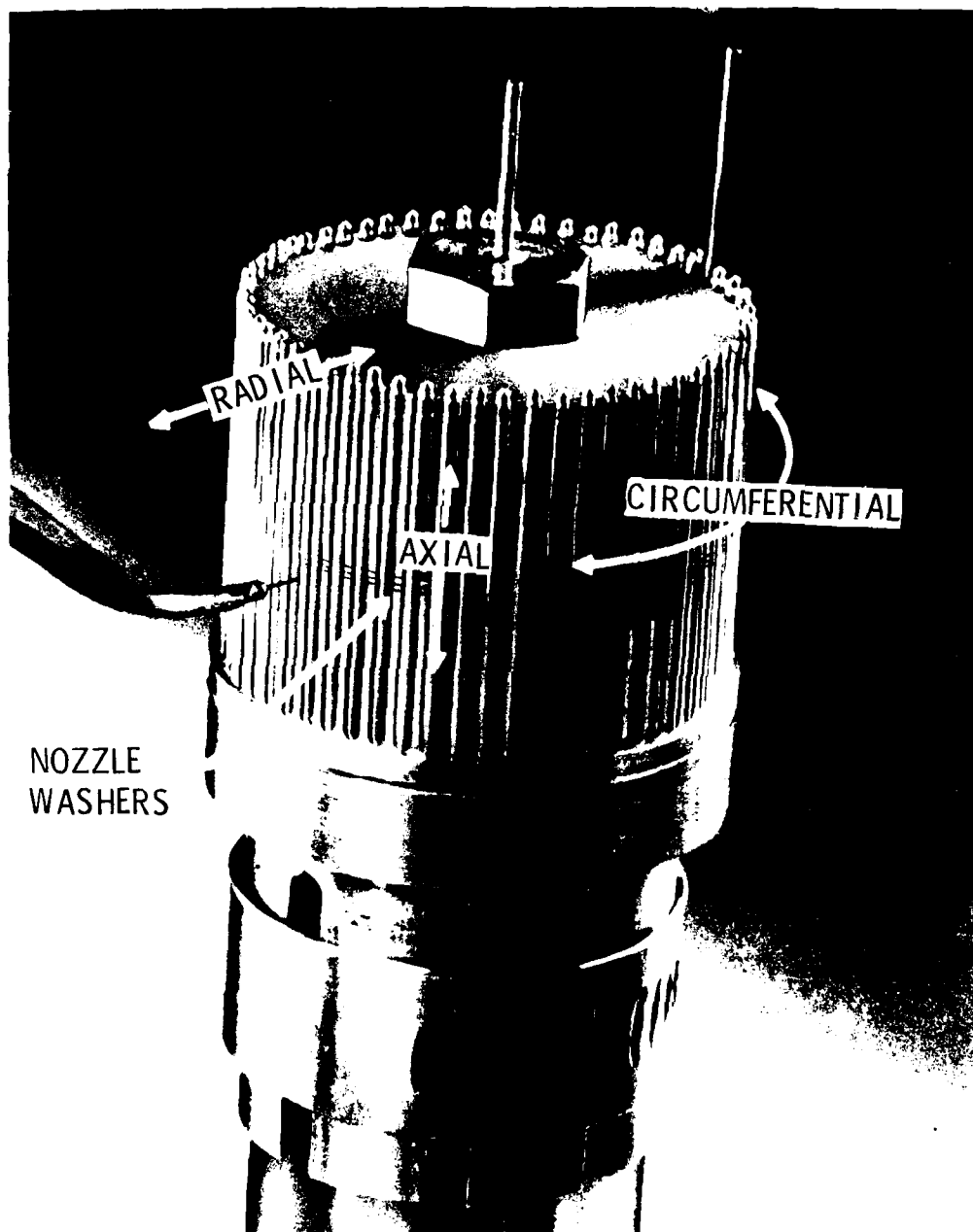


Figure 12. Sample Nozzle for Core Flow Tests

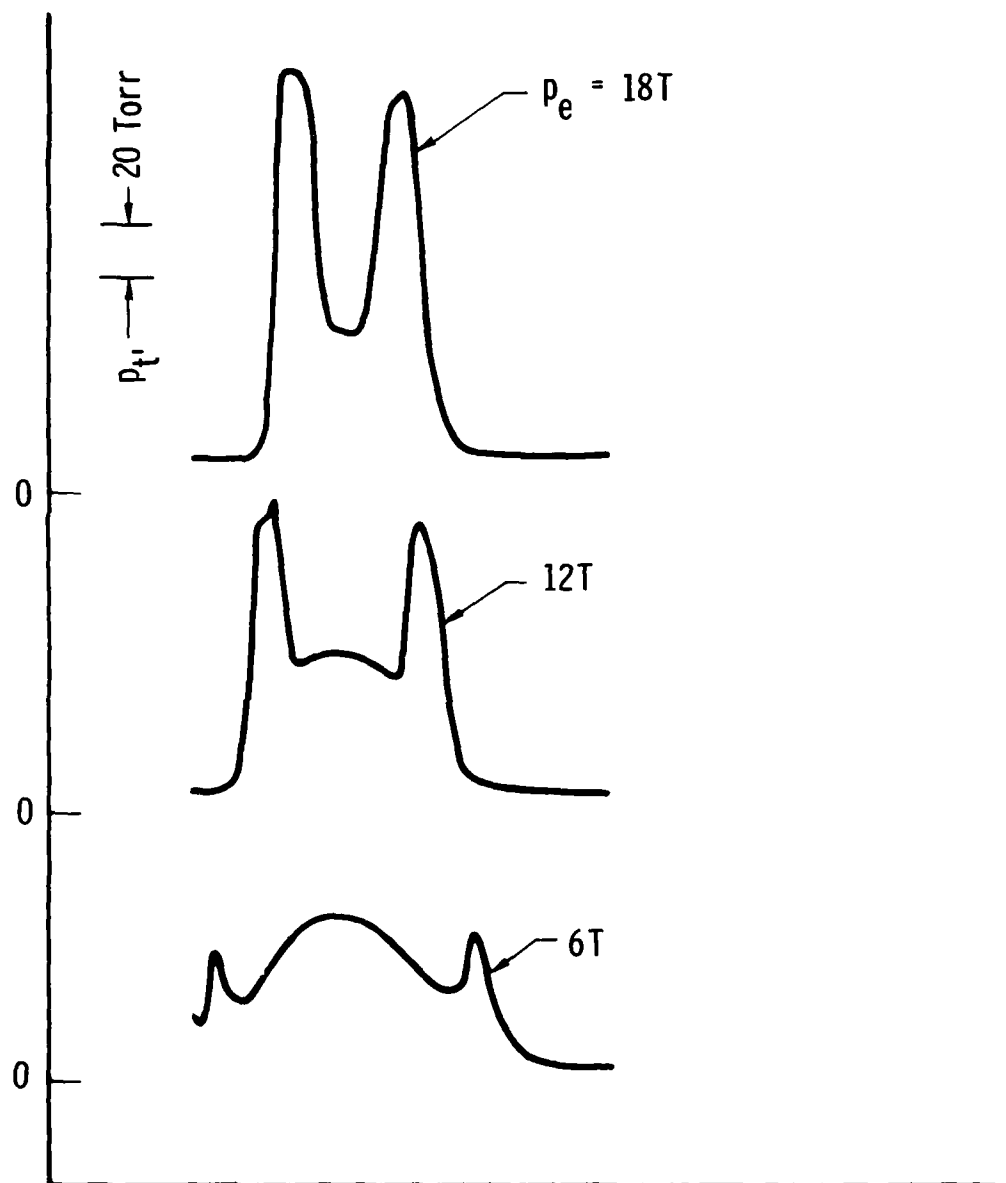


Figure 13a. Axial Scan Across Oxidizer Jet;
 $R = 1 \text{ mm}$, $p_o = 1 \text{ atm}$

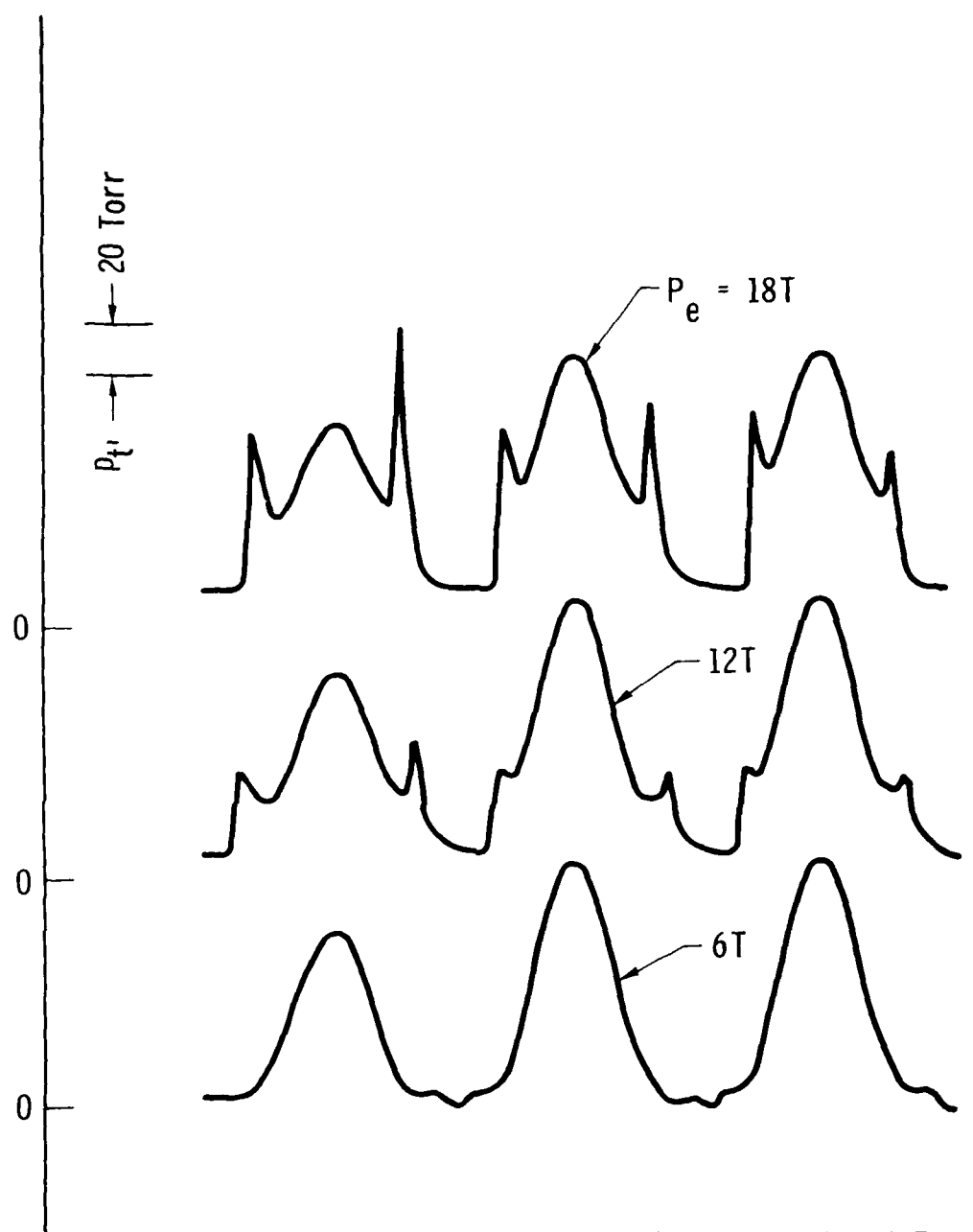


Figure 13b. Axial Scan Across Fuel Jet; $R = 1 \text{ mm}$, $p_o = 1 \text{ atm}$

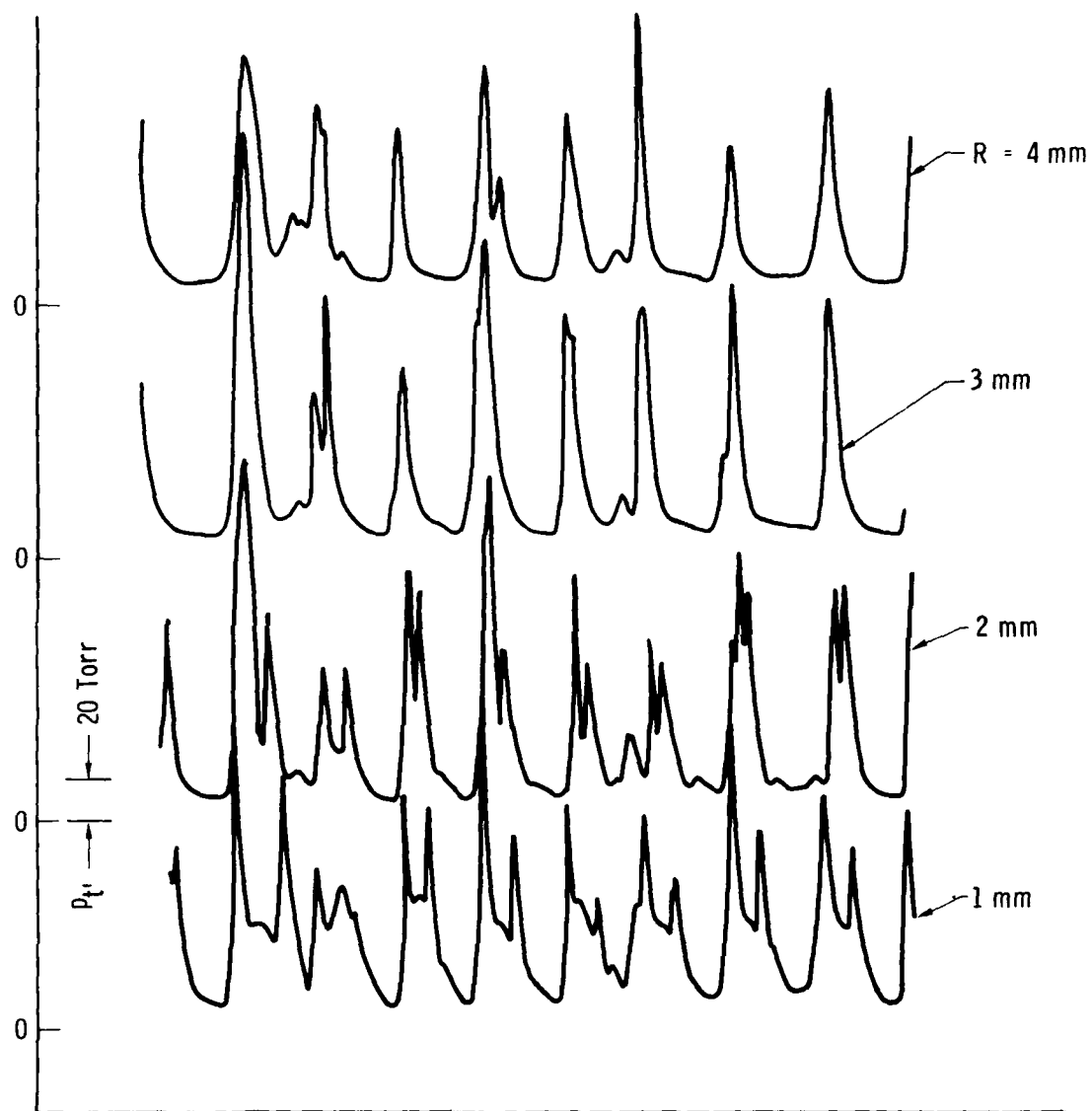


Figure 14. Circumferential Scan Around Oxidizer Jets; $p_o = 1 \text{ atm}$, $p_e = 12 \text{ Torr}$

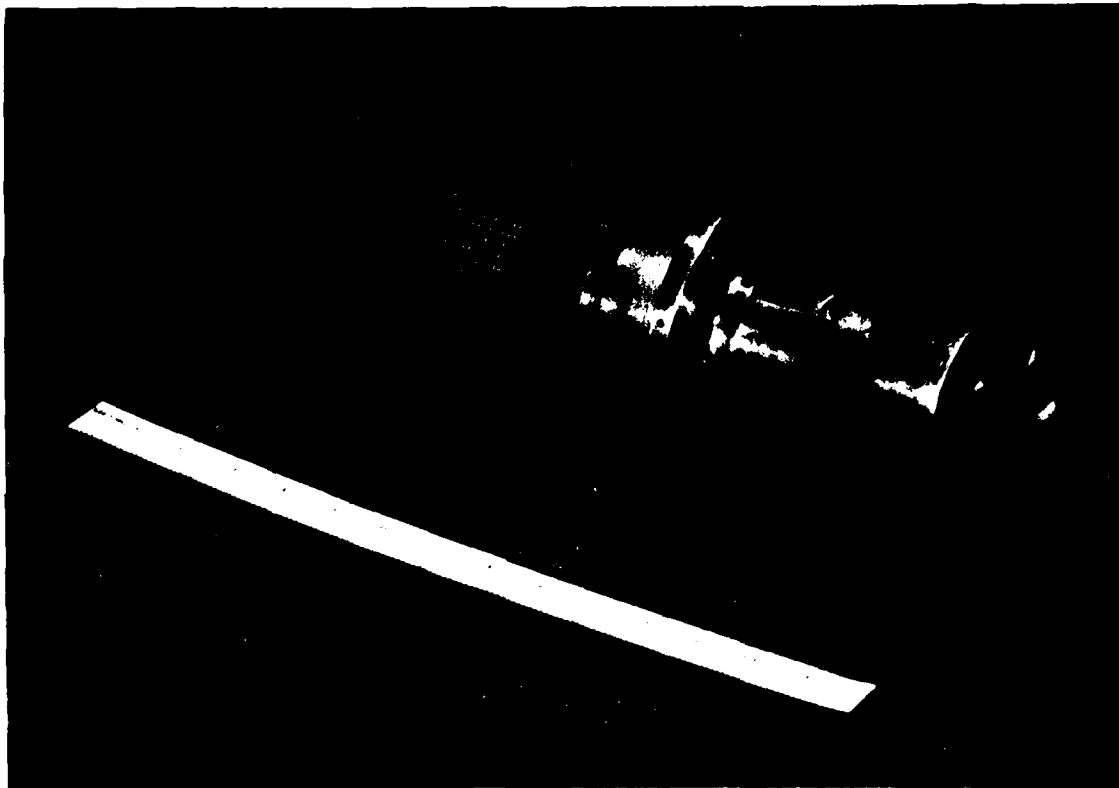


Figure 15. Nozzle Assembly

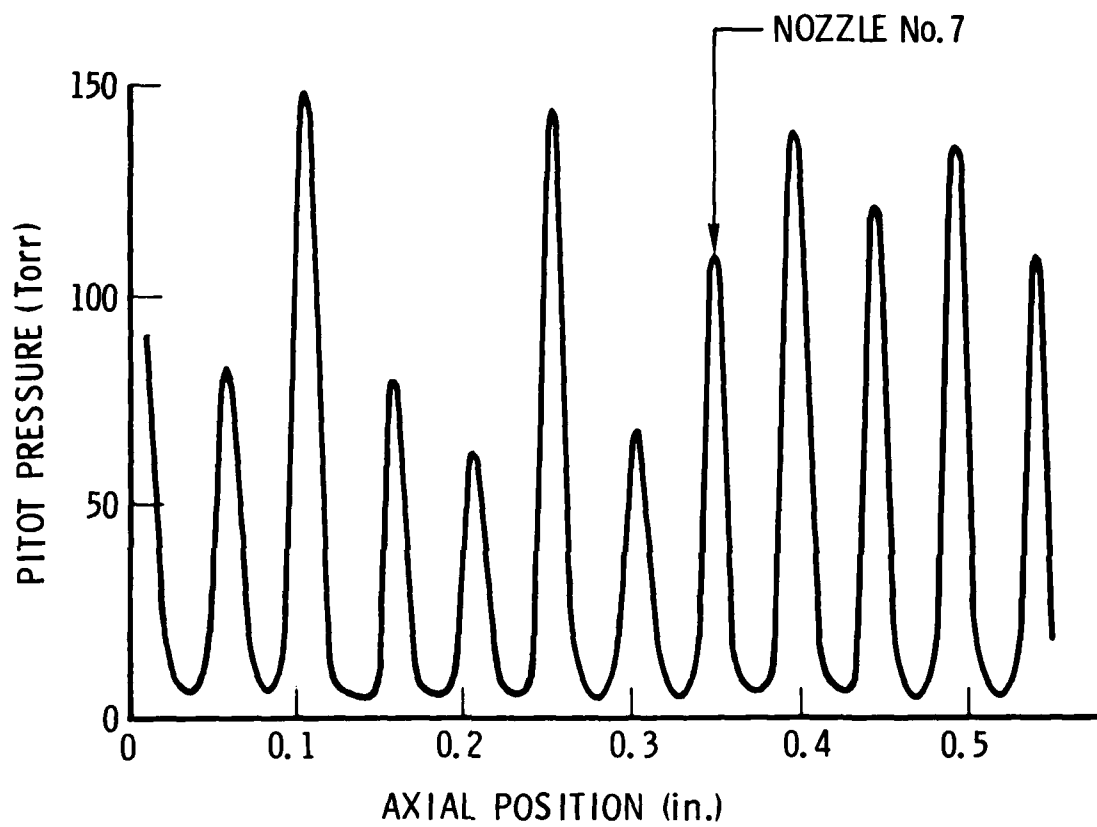


Figure 16. Cold Flow Test, Axial Pitot Pressure Scan at $R = 0.5$ mm

VI. HOT FLOW TESTS

A plenum temperature of 800 K was originally to be obtained by heating the diluent (in this design, nitrogen) to a temperature of approximately 1200 K in a resistance heater and mixing with gaseous fluorine. This mixture would be passed through a heat exchanger to heat the hydrogen entering the fuel manifolds so that there would not be a temperature gradient along the length of the nozzle. The final temperature of the gases in the plenum would be 800 K at a pressure of 1 atm. Initial tests with nitrogen substituted for fluorine revealed that these plenum conditions could be achieved (Figure 17). However, there was a significant gradient in the temperature of the flow from one end of the nozzle to the other, and the stagnation temperatures in the flow were considerably lower than in the plenum. These factors indicated that the preheating of the hydrogen was inadequate. During the hot, nonreacting flow tests, the heater used to heat the nitrogen failed twice, once in a minor incident and finally with a major failure in the chamber insulator (Figure 18).

As mentioned previously, it was expected that NO would be required to initiate the reaction because the F-atom concentration at 800 K and 1 atm is extremely small. This, together with the wide separation of the fuel and oxidizer in the nozzle design, would make ignition difficult if not impossible. Tests on the program up to this point had not used any NO because of increasing resistance from the health and safety offices against releasing small amounts of NO/NO₂ into the atmosphere. The scrubber on the laser facilities, although effective for HF and F₂, does not remove NO_x.

Because of this restriction and the problems encountered with the heater, it was decided to use combustion to heat the gases in the plenum. It was hoped that there might be some nonequilibrium F-atoms left over from the combustion that would serve as the reaction initiator. Figure 19 is a schematic of the combustor. The reactants are injected through six doublets in a small chamber separate from the nozzle plenum. A small amount of deuterium is mixed with all the fluorine and reacts with essentially no diluent. (A small amount of nitrogen is injected with the D₂ to serve as a purge to prevent F₂

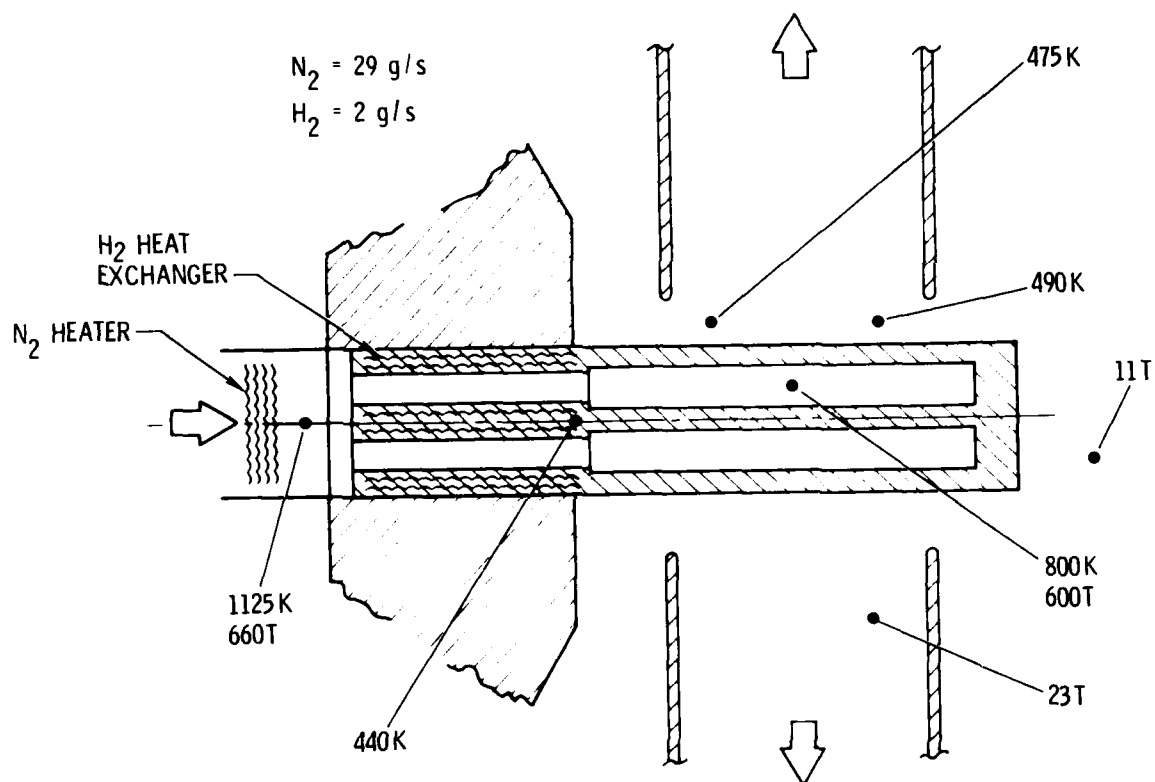


Figure 17. Nonreacting Flow Conditions



Figure 18. Nitrogen Heater

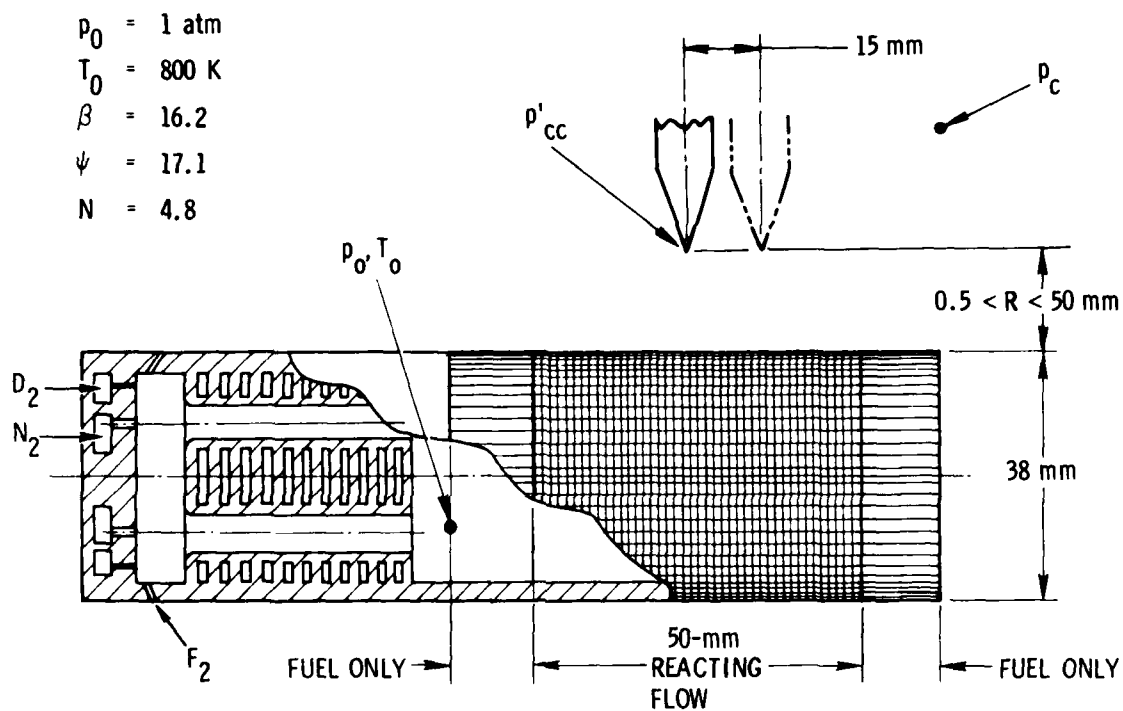


Figure 19. Combustor-Nozzle Configuration

from ever getting into the feed lines.) The nitrogen diluent is then mixed with the combustion gases while passing through the heat exchanger for the fuel. A nickel-sheathed, chromel-alumel thermocouple measures the temperature of the gases in the plenum.

VII. REACTIVE FLOW TESTS

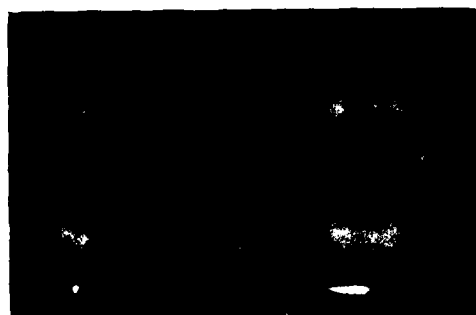
With the use of the combustor configuration, a series of reactive flow tests were undertaken. The nominal operating conditions are listed in Figure 19. It was apparent from the beginning that there were sufficient F-atoms left over from the combustion to reliably initiate the reaction in the flow out of the nozzle. If the D_2 was not injected at the start of a run, there would be no reaction in the nozzle flow, but often a detonation occurred downstream in the exhaust system. If the D_2 was turned off during a run, the reaction in the nozzle flow stopped, but reaction continued on hot parts downstream.

Initial tests with the compression chamber in position around the nozzle (Figure 1) did not reveal any evidence of a shock structure in the flow as observed through viewing ports in the chamber. Rather, the flow appeared to be impeded by the chamber with a large portion of it turning to exit from the openings at each end. The compression chamber was removed, and the nozzle permitted to exhaust directly into the test section (approximately 35 cm wide by 35 cm high by 60 cm long). A definite layering was then observed in the flow as shown by the photographs in Figure 20. These pictures were taken with ASA 800 Ektachrome film with a 1-sec exposure at f 1.8. The two images are formed by a mirror system that permits half of each frame to show the end view and the other half the side view of the nozzle. The color of the chemiluminescent flow is a pale orange in the inner region (end view) with a bright orange layer (shock?) surrounded by a region of decreasing orange brightness as the flow expands. The radial position of the luminous layer is a function of the back pressure established by throttling the exhaust leaving the test section (Figure 20).

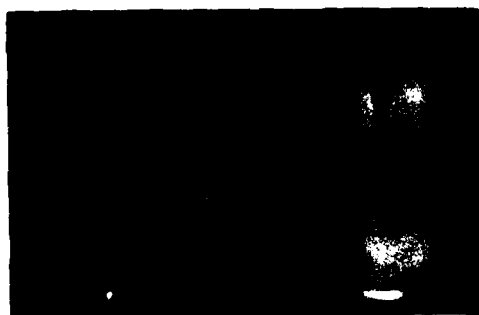
Infrared video pictures taken of the flow field at 30 frames/sec indicated that the position of the layered structure is stable in time and, in general, moves in a steady manner as the back pressure is changed. There does appear to be hysteresis in local areas of nonuniform flow as the pressure is reduced and the layer moves out. The layer at these locations appears to



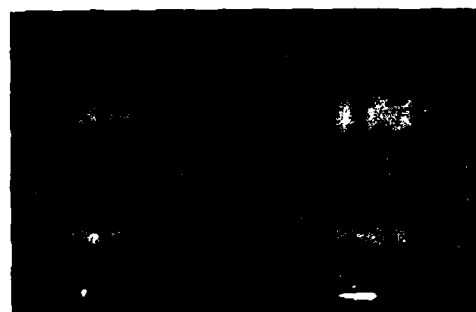
p_c (Torr)



17.6



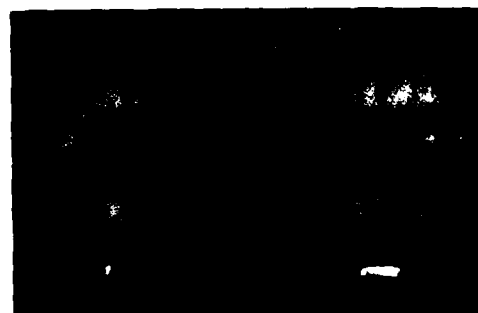
13.2



19.6



15.0



22.6

Figure 20. Chemiluminescence Photographs

"jump" to stable positions rather than move in a steady manner. These visual observations indicate the layer has characteristics that could be associated with a complex shock-wave structure. That is, the position of the shock layer is established by back pressure, its movement with back pressure indicates hysteresis that is typical of shock systems, and the side view of the layer is what one would expect the shock shape to be, considering end effects.

Although the evidence of chemiluminescence is qualitatively correct for the existence of a normal shock, several measurements were made in the flow to provide quantitative evidence.

VIII. PRESSURE MEASUREMENTS

As mentioned before, it was planned that the existence of a normal shock could be confirmed by pitot-pressure measurements in the radial flow. However, the presence of large nonuniformities and the small extent of the undisturbed supersonic flow from the nozzle jets made the pitot-pressure measurements difficult to interpret. For example, Figure 21 indicates the pitot pressure measured 2 mm from the surface of the nozzle with the use of a probe of 0.25 mm diameter to scan axially the center region of the cylindrical nozzle. In Figure 22 is shown the pitot pressure in a radial scan above oxidizer nozzle jet 7 for the same flow conditions.

It appears that there are three regions in the radial flow in which the pitot-pressure results require different interpretation. In Figure 22 the region from the nozzle surface to a radial position of 1.5 to 2 mm is dominated by the behavior of individual jets. Using the results of the cold-flow tests (Figure 13), one can characterize the oxidizer and fuel orifices as shown in Figure 23a and 23b, respectively. Considering the large divergence in the flow from both of these jets, it is expected that they would expand into the area between them at a very short range (i.e., 1.5 to 2 mm). This explains the sharp drop in pitot pressure measured within a distance of 1.5 mm during the radial scan (Figure 22).

Beyond 1.5 to 2 mm, the jets appear to interact, and there are resultant peaks in the pitot pressure observed in both the radial scan and axial scan (Figure 21). If this is the case, the diffusion process has already begun, and the static pressure is increasing, but with some loss in the total pressure as a result of the interaction shock losses.

The data taken during axial scans over the region from 2 to 14 mm were averaged using a PDP11 computer, and these results are plotted in Figure 24 as average pitot pressure versus radial position. The average pitot pressure approximates the value for the individual jets at 2 mm and then decreases monotonically with radius, as one would expect for a radially expanding supersonic flow. The curvature downward could be the result of total pressure

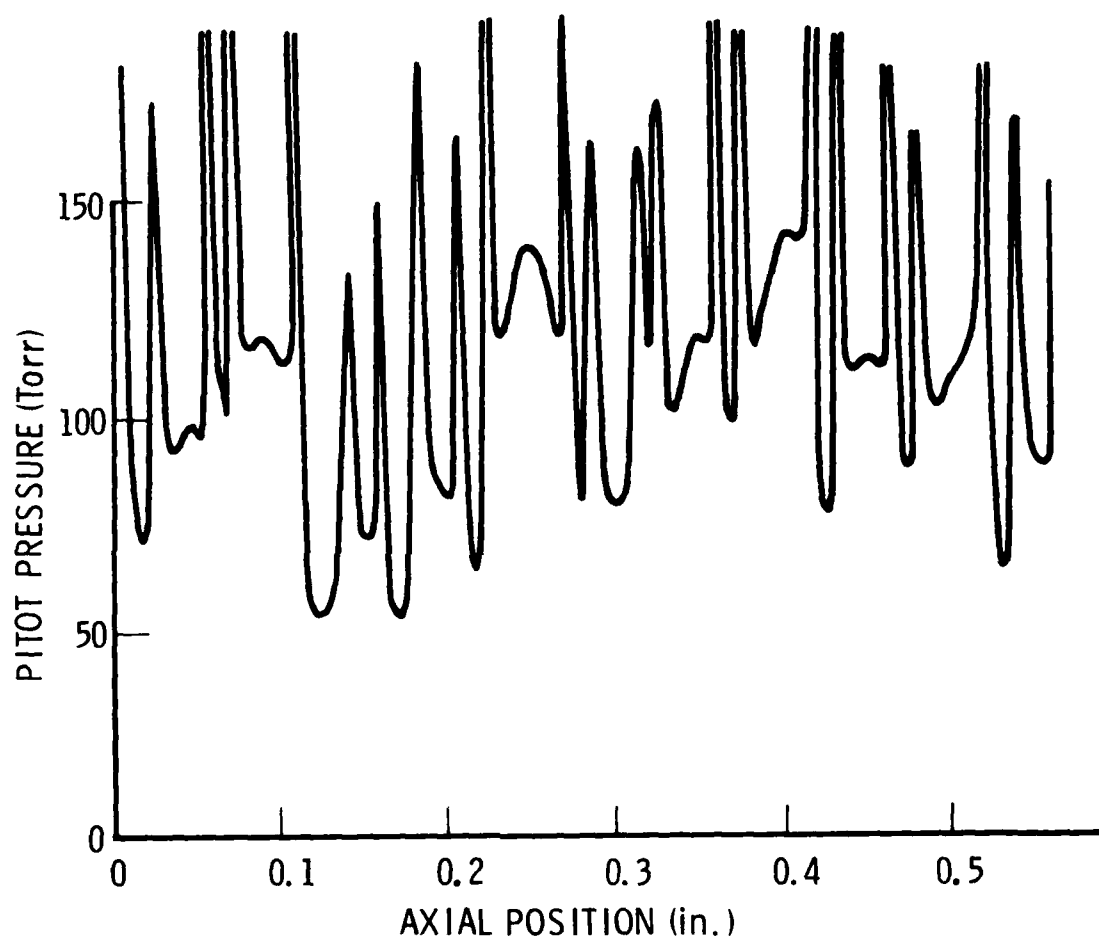


Figure 21. Reacting Flow Test, Axial Pitot Pressure Scan at $R = 2$ mm

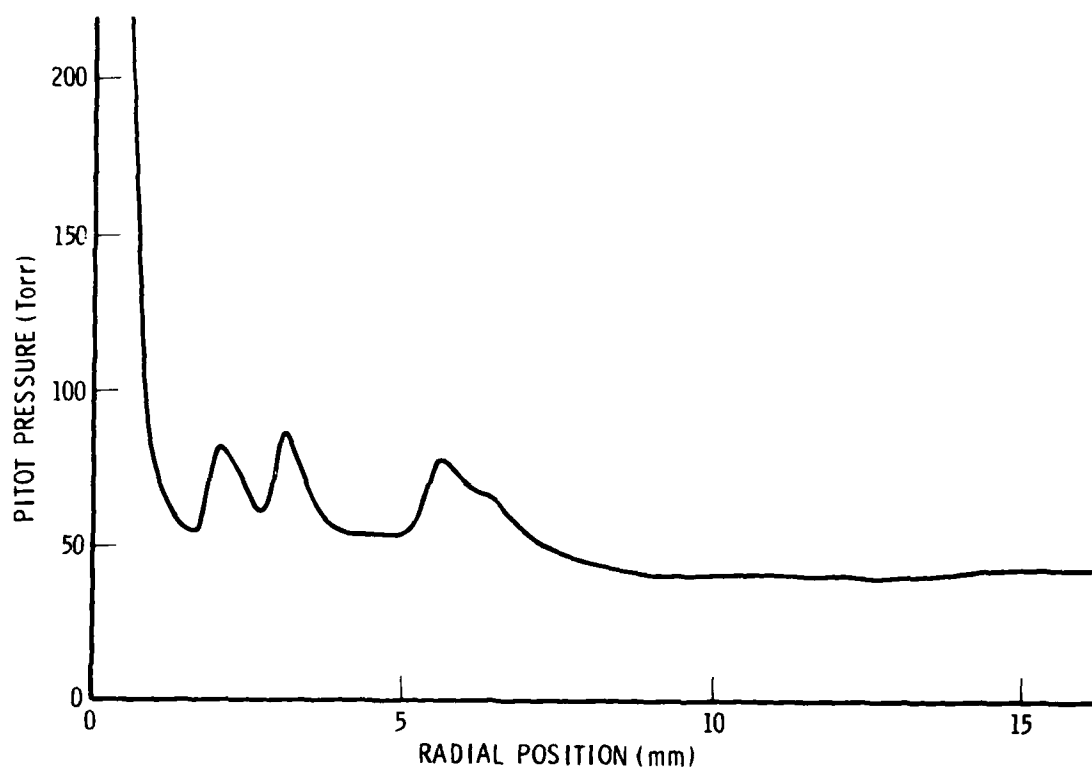


Figure 22. Pitot Pressure Above nozzle No. 7, $p_c = 14$ Torr

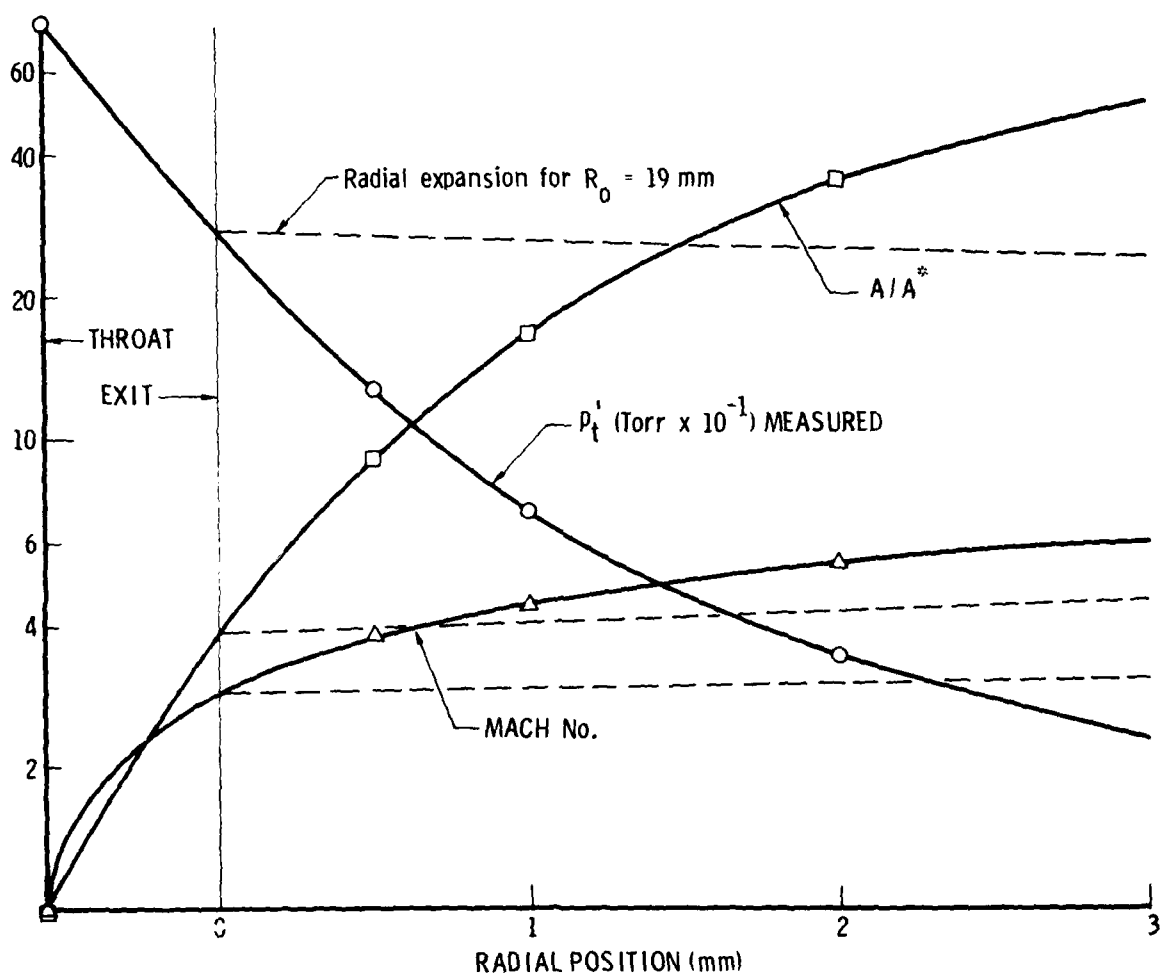


Figure 23a. Oxidizer Nozzle Characteristics, $\gamma = 1.4$

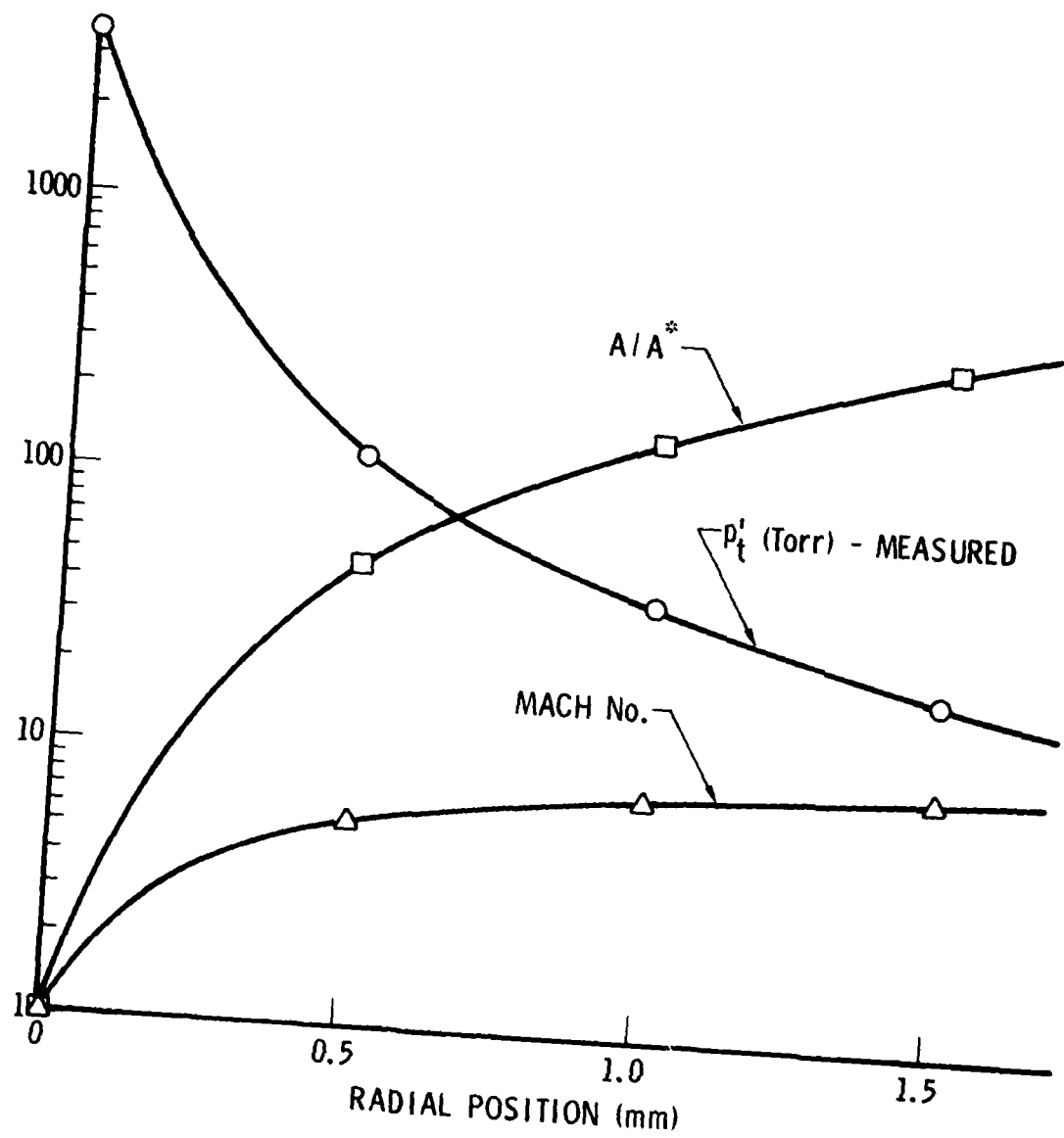


Figure 23b. Fuel Nozzle Characteristics, $\gamma = 1.4$

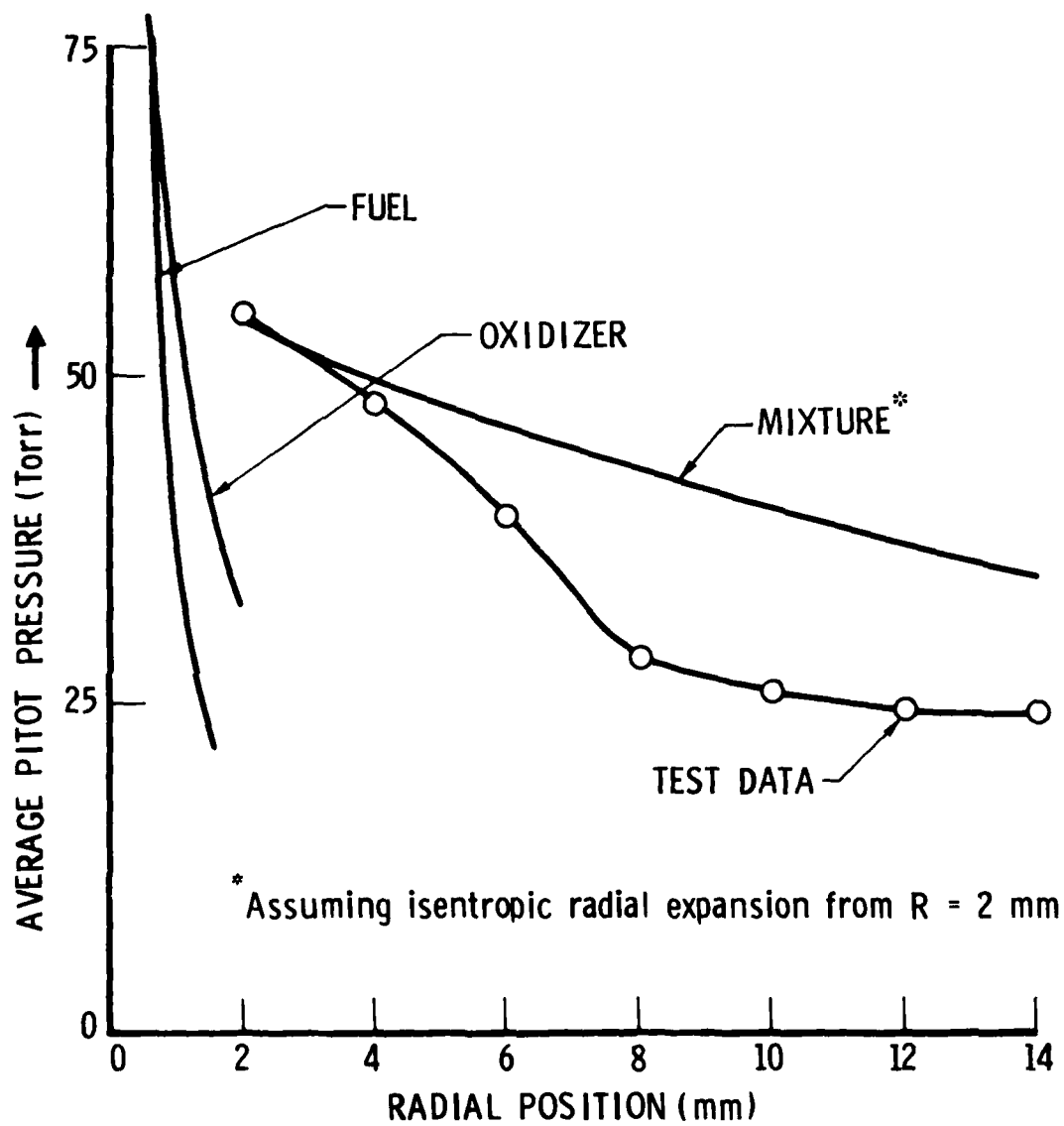


Figure 24. Computer Averaged Results, $p_c = 14$ Torr

loss resulting from successive interaction shock losses. It is evident from the radial scan on nozzle 7 (Figure 22) that there is a shock train. However, the error bars on the average pitot-pressure results are of the order of 10 Torr wide, so not too much significance should be ascribed to curvature.

The third region in which the pitot pressure has still another interpretation lies beyond approximately 10 mm. In this region, the large nonuniformities observed in the axial scans are virtually gone, and the change of pitot pressure with radial position is greatly reduced (Figures 22 and 24). Because this is the region in which the luminous layer also appears in the flow with a back pressure of 14 Torr, one is lead to the conclusion that a normal shock has occurred: the flow is hot and subsonic, the reaction rates are greatly increased, and the nonuniformities are smeared away.

The pitot-pressure measurement was also used to confirm that the flow as a whole in the region inside the normal shock was supersonic. This was done by observing the "zone of silence" that exists as the back (downstream) pressure was increased. The pitot probe was fixed at a particular radial position, and the back pressure was increased until the pitot-pressure reading changed. The results of this "pressure scan" are shown in Figure 25 where the back pressure at which the pitot pressure is influenced, the critical pressure, is plotted against radial position. Two cases are shown, the probe in line with nozzle 7 and then moved to the space between nozzles 7 and 6 (i.e., a base region). Note that both locations give the same critical pressure except at the inner radial positions, indicating that the flow as a whole is supersonic and acts as a more-or-less uniform flow field. Incidentally, the "zone of silence" results give shock locations as a function of back pressure very similar to the photographs of the chemiluminescent layer. About a 3-Torr difference in pressure level does exist between the "zone" and layer positions, which could be attributed to differences in the dynamic pressure component of the "static" pressure measurement made with different instrumentation at different locations for the two test series. In addition, the exact back pressure at which the pitot pressure was disturbed at the larger radial positions was difficult to select because the disturbance there was relatively small (i.e., flow already somewhat diffused).

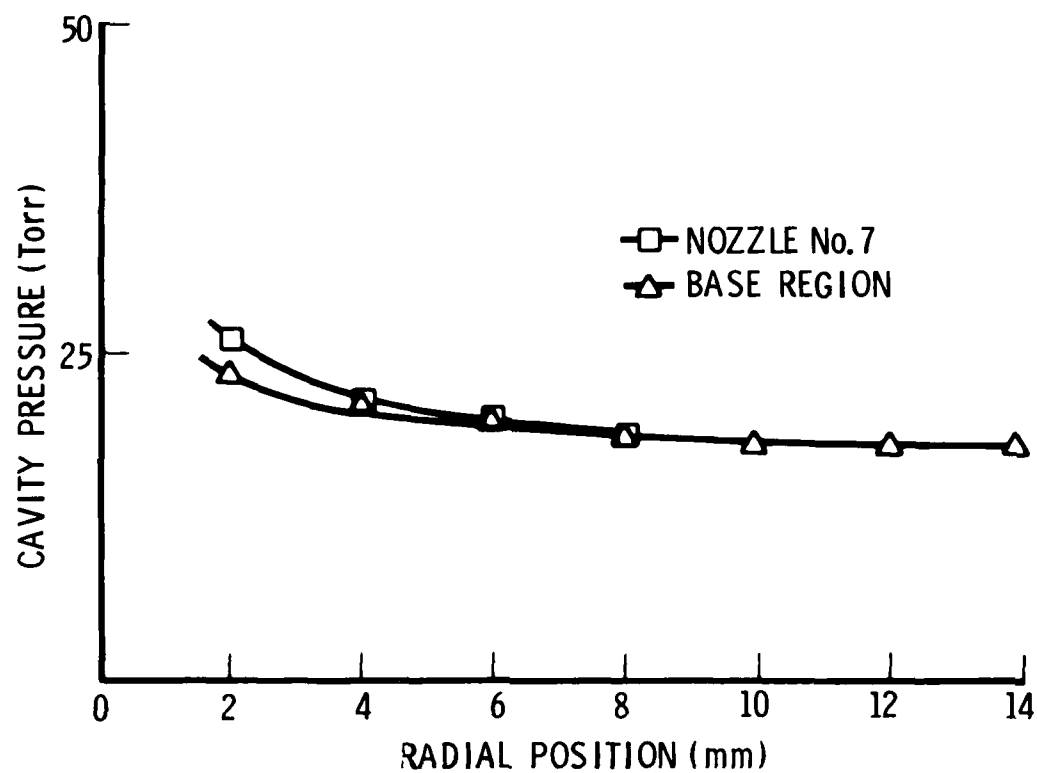


Figure 25. "Zone of Silence" Results

Having verified that the inner region is supersonic, a pitot-static measurement was made downstream of the shock layer to verify that the flow here is subsonic. Because the flow in this region is quite uniform, a larger probe could be used (Figure 26). Four static-pressure ports are located on a 5-deg wedge, and three total pressure ports are located on the opposite side approximately 0.5 mm from the sharp leading edge. Data were taken with a single transducer in a Scanivalve. Radial scans with the probe were made slowly to minimize transients in the tubulations to the Scanivalve. The results of these measurements are shown in Figure 27 where Mach No. is plotted against radial position. As expected, the flow is subsonic. The subsonic diffusion that should occur as the flow expands radially is offset by the change in flow area in the axial direction that is evident from the chemiluminescence in the side view photographs (Figure 20).

Note that the Mach No. behind the shock is quite high (0.95), implying that the Mach No. of the flow immediately upstream of a normal shock is low ($M_1 \times M_2 = 1$, $M_1 = 1.05$). Therefore, the static-pressure rise across the shock is very small (2 Torr). This is consistent with the small disturbances observed in the "zone of silence" tests. The dashed curves in the supersonic region of Figure 27 are estimates based on pitot-pressure data and the 6-Torr static pressure measured at the surface of the nozzle.

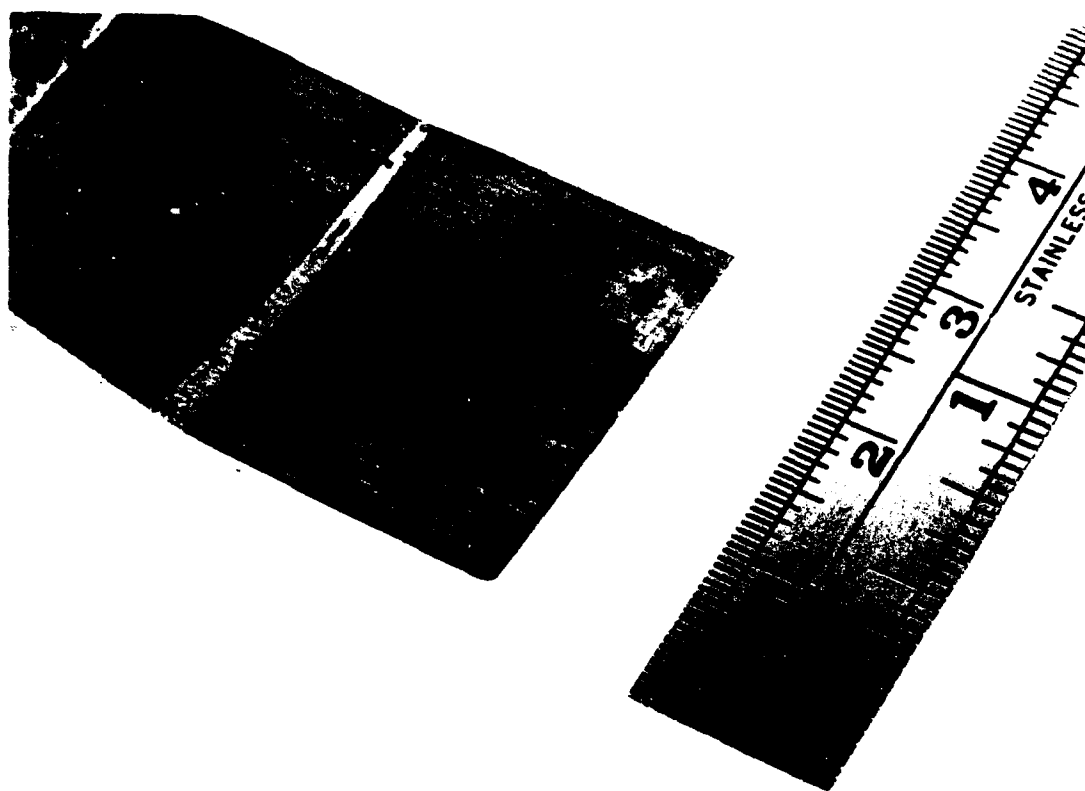


Figure 26. Pitot-Static Pressure Probe

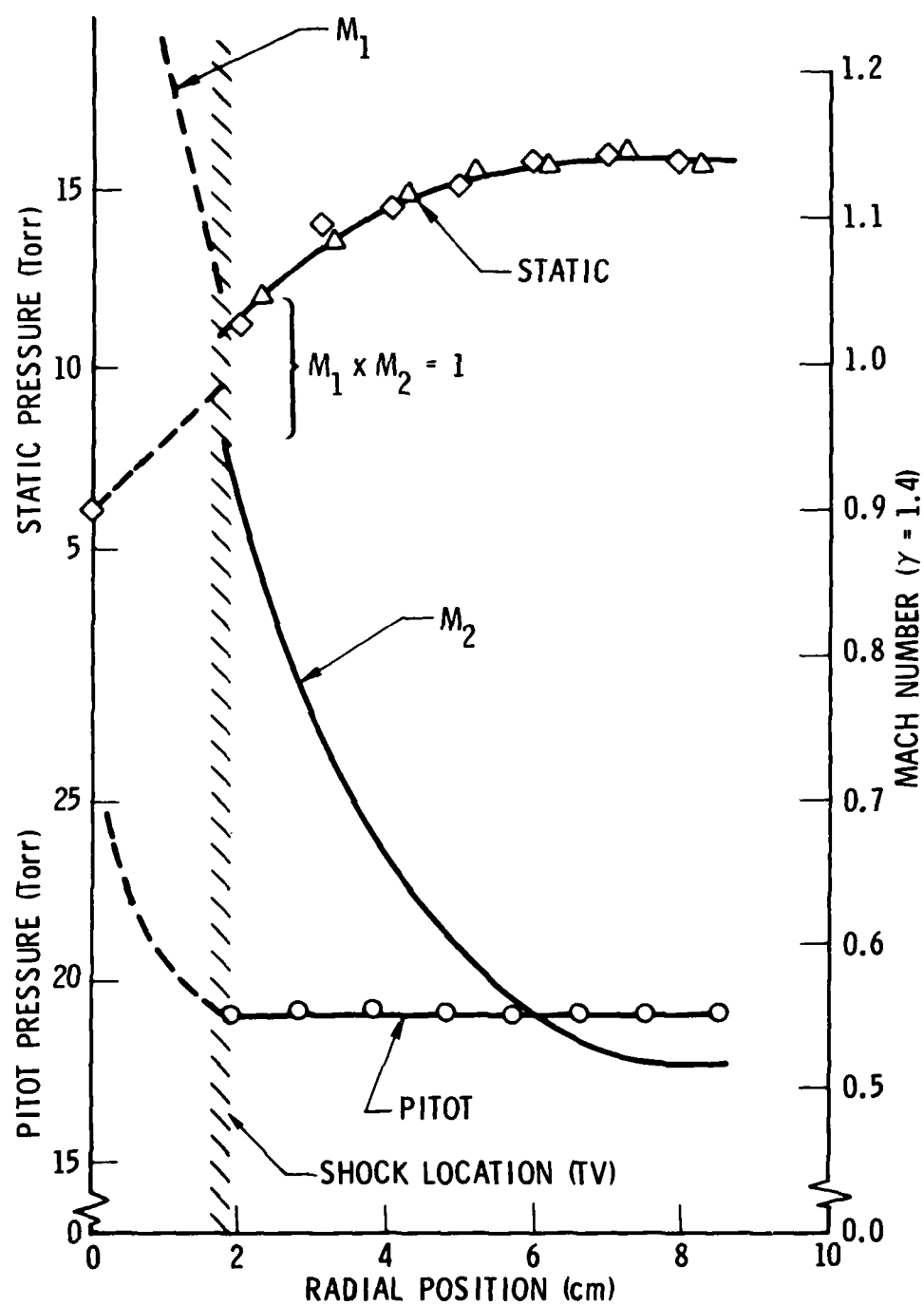


Figure 27. Results of Pitot-Static Measurements

IX. TEMPERATURE MEASUREMENTS

Although the pressure measurements appear to be conclusive in establishing that a stable, normal shock exists in the flow, additional evidence was desired. A series of tests were carried out in which the rotational temperature of the flow as a function of the radial position was evaluated from the J-distribution of the $v = 3$ state of HF.⁶ In addition, the relative population of the HF($v = 3$) state as a function of radial position would also be indicative of the rate and extent of the reaction on the chain. The setup for these tests is shown in Figure 28; the results are given in Figure 29.

Both the temperature and the HF($v = 3$) population increase at the location of the shock as observed by IRTV. The drop in temperature downstream is believed to be associated with the mixing of the reacting flow with the hydrogen layer that is flowing on both sides (Figure 19). An unshielded thermocouple placed in the reacting flow at a radial position 3 cm from the nozzle (90 deg away from the radial scan of the spectrograph) recorded approximately 1100 K. This temperature is nearer the value that one would expect for the completely reacted flow (1250 K).

⁶M. A. Kwok, S. J. Spencer, and R. W. F. Gross, Chemiluminescence from the Supersonic Jet of a CW He Chemical Laser, J. Appl. Phys. 45 (8) (August 1974).

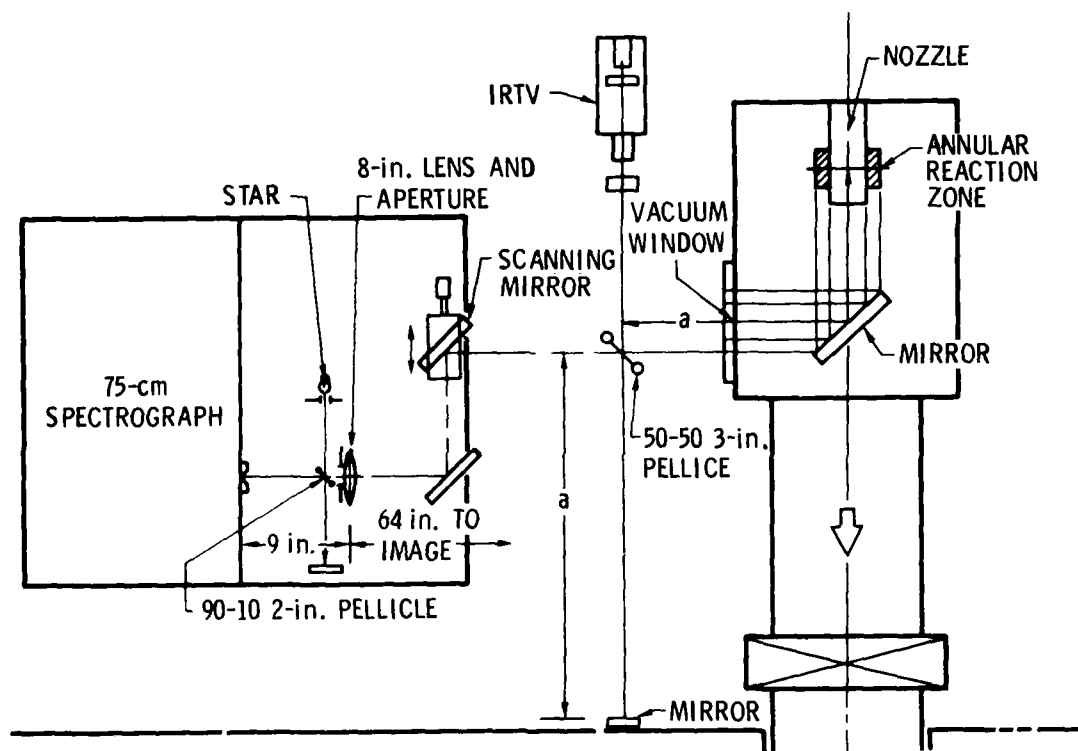


Figure 28. Rotational Temperature Test Setup

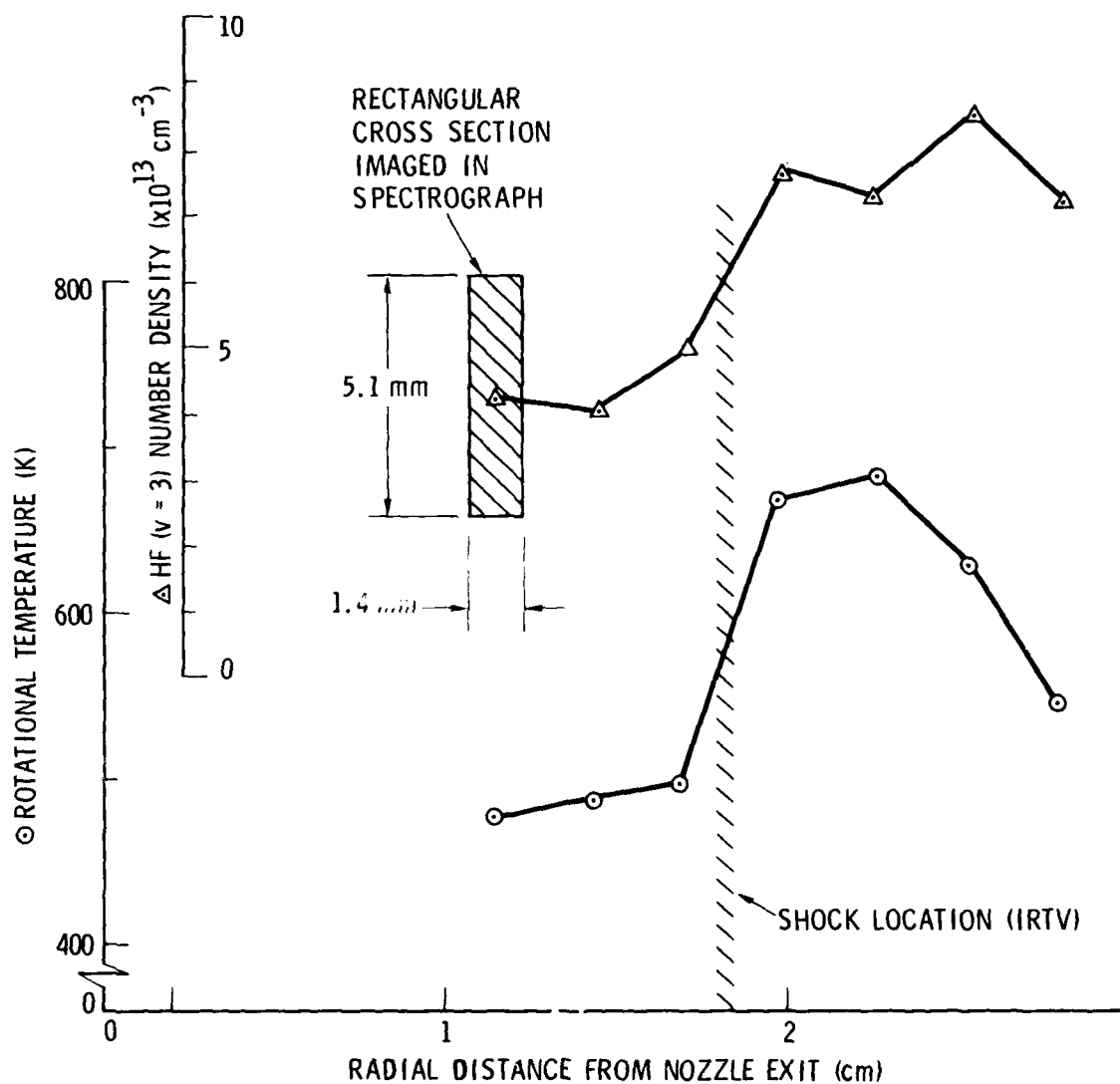


Figure 29. Rotational Temperature and HF($v = 3$)
 $[T \pm 50\text{K}, \text{ relative HF}(v = 3) \pm 10\%]$

X. CONCLUSIONS AND RECOMMENDATIONS

A small-scale reacting radial flow has been generated that is similar to the flow expected in large-scale HF(DF) cylindrical lasers. Heat release in the flow is obtained from the chain reaction, and large flow nonuniformities are present because of a rather simple nozzle design.

The flow is readily visualized because of the chemical reactions that occur and can be photographed with high-speed color film and recorded on a highly sensitive video-tape system. Photographs reveal a shock structure that is stable and that can be located at any radial position by setting the downstream pressure into which the flow exhausts. Video records indicate that the shock has temporal stability and exhibits the hysteresis phenomena with pressure changes that are characteristic of shock systems.

Pitot-pressure measurements indicate that the flow upstream of the shock is supersonic and quite nonuniform. Pitot-static-pressure measurements downstream of the shock reveal that the flow is subsonic, with the Mach No. decreasing as the distance from the nozzle increases. Rotational temperature measurements using a spatial, spectral scanning spectrograph indicate that the static temperature increases sharply at the position of the shock as does the production of HF($v = 3$).

Most pressure and temperature data were taken with the shock located at a radial position approximately 2 cm from the nozzle. At this location, the shock is stable and appears to be relatively weak with an upstream Mach No. of 1.05 to 1.10. Although the initial Mach No. of the primary and secondary jets is much higher, we believe the low Mach No. at 2 cm is the result of large shock interaction losses associated with the flow into large base regions of this particular nozzle and/or mixing with low-momentum flow "leaking" into these areas because of the mechanical type of assembly of the nozzle.

Because the relatively weak shock observed here is definitely stable, we expect that higher Mach No. flows involving stronger shocks would also be stable. This is expected because the loss of total pressure across a normal

shock increases with the Mach No. of the flow, thereby "stiffening" the shock to any disturbing effects such as nonuniformities in the flow or rapid chemical reactions that heat the flow. In fact, in this experiment, when the back pressure was increased so the shock moved in to regions of higher Mach No., greater flow nonuniformities and increased unreacted chemistry, the stability of the shock as observed with IRTV appeared to be unaffected.

In view of the results obtained in this small-scale experiment, we believe that it is feasible to operate a cylindrical, chemical laser without a supersonic diffuser and to obtain 100% of normal shock recovery with no loss in laser efficiency.

Therefore, we recommend that additional tests be performed to verify these results in a mid-scale and full-scale facility. In Figure 30, we show schematically the arrangement for an experiment with a medium-size laser in which all the properties of the typical cylindrical laser can be incorporated. The gain region would be of sufficient size to permit flow diagnostics and also to study laser operation with annular optics. In addition, the question of end effects on the flow and optics enclosures could be addressed, and the actual pressure recovery of the system to the point of a subsonic duct outlet(s) could be measured.

When, and if, one should become available, a large-size laser would give the opportunity to further evaluate these concepts at practical flow dimensions.

The practical advantages of the free-standing normal shock-layer pressure-recovery concept for cylindrical laser geometries follow:

1. It eliminates the need for the massive aerodynamic diffuser hardware usually associated with high-energy-laser pressure-recovery systems. This will be of importance in airborne applications where weight and volume are crucial systems parameters and, also, in the ground testing of large-scale, low-pressure lasers where the pumping limitations of exhaust systems require a maximum pressure level of their inlet gases.
2. It produces the pressure recovery across a thin shock layer rather than across a long (in the radial direction) diffuser structure where, for a cylindrical laser, the exit area is much larger than

$$A_{\text{NOZZLE}} = 400 \text{ in.}^2$$

$$A_e/A_s = 1, A_c/A^* = 3, L_{\text{lasing}} \leq 2 \text{ in.}$$

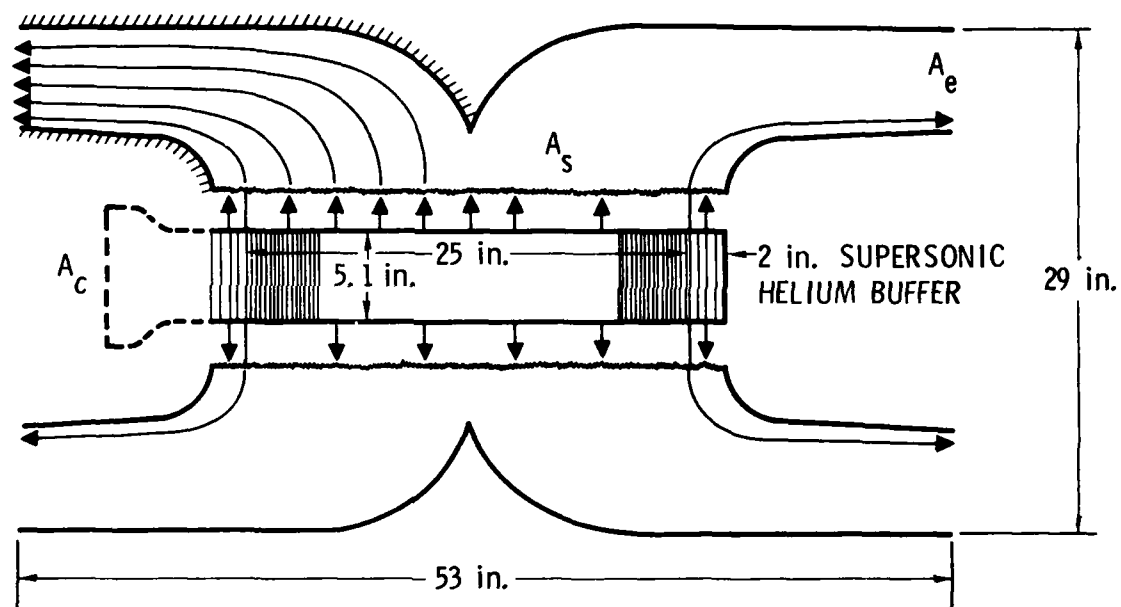


Figure 30. Cylindrical Chemical Laser Cylindrical Shock Pressure Recovery

the inlet area. This area effect difference (from a simple analysis of the governing conservation equations) provides a 20 to 40% advantage in potential pressure recovery to the normal shock concept, depending on laser size and design.

3. It essentially is an unstarted supersonic wind tunnel process. That is, when the laser device is started against a given back pressure, the shock front moves through the nozzles, across the laser cavity region, and to its final position as the laser device mass flows and pressures rise to their operating levels. However, for a device with a diffuser, the shock wave has to be forced through the diffuser (the second throat in the wind tunnel analogy) before the diffuser can achieve its maximum performance. Typically, for a non-variable area diffuser structure, this requires a short-duration over-pressure ratio of a factor of 2 in the flow system. If the laser is exhausting into a vacuum system, this can be accomplished by evacuating the exhaust duct originally to half the final operating pressure. However, if the laser is exhausting to the atmosphere, the over-pressure has to be provided by the laser plenum chambers and gas supply systems. In either case, this illustrates a significant advantage of the normal-shock-layer concept.

The normal-shock-layer pressure-recovery concept need not be limited to cylindrical laser geometries. That is, the flow from any laser geometry with a supersonic medium (e.g., a linear bank) can be given enough radial properties, including treatment of the boundary flows, so that it would support a stable normal shock layer at, or downstream of, a specified station. Thus, we believe that this concept has a universal utility of significance in the high-power continuous-wave laser field.

LABORATORY OPERATIONS

The Laboratory Operations of The Aerospace Corporation is conducting experimental and theoretical investigations necessary for the evaluation and application of scientific advances to new military concepts and systems. Versatility and flexibility have been developed to a high degree by the laboratory personnel in dealing with the many problems encountered in the Nation's rapidly developing space systems. Expertise in the latest scientific developments is vital to the accomplishment of tasks related to these problems. The laboratories that contribute to this research are:

Aerophysics Laboratory: Aerodynamics; fluid dynamics; plasmadynamics; chemical kinetics; engineering mechanics; flight dynamics; heat transfer; high-power gas lasers, continuous and pulsed, IR, visible, UV; laser physics; laser resonator optics; laser effects and countermeasures.

Chemistry and Physics Laboratory: Atmospheric reactions and optical backgrounds; radiative transfer and atmospheric transmission; thermal and state-specific reaction rates in rocket plumes; chemical thermodynamics and propulsion chemistry; laser isotope separation; chemistry and physics of particles; space environmental and contamination effects on spacecraft materials; lubrication; surface chemistry of insulators and conductors; cathode materials; sensor materials and sensor optics; applied laser spectroscopy; atomic frequency standards; pollution and toxic materials monitoring.

Electronics Research Laboratory: Electromagnetic theory and propagation phenomena; microwave and semiconductor devices and integrated circuits; quantum electronics, lasers, and electro-optics; communication sciences, applied electronics, superconducting and electronic device physics; millimeter-wave and far-infrared technology.

Materials Sciences Laboratory: Development of new materials; composite materials; graphite and ceramics; polymeric materials; weapons effects and hardened materials; materials for electronic devices; dimensionally stable materials; chemical and structural analyses; stress corrosion; fatigue of metals.

Space Sciences Laboratory: Atmospheric and ionospheric physics, radiation from the atmosphere, density and composition of the atmosphere, aurorae and airglow; magnetospheric physics, cosmic rays, generation and propagation of plasma waves in the magnetosphere; solar physics, x-ray astronomy; the effects of nuclear explosions, magnetic storms, and solar activity on the earth's atmosphere, ionosphere, and magnetosphere; the effects of optical, electromagnetic, and particulate radiations in space on space systems.